AD NUMBER

AD458348

LIMITATION CHANGES

TO:

Approved for public release; distribution is unlimited.

FROM:

**Distribution authorized to U.S. Gov't. agencies and their contractors;
Administrative/Operational Use; MAR 1965. Other requests shall be referred to Air Force Engineering Development Command, AEDC-IN (STINFO), 251 First Street, Arnold AFB, TN 37389-2305.**

AUTHORITY

AEDC Itr, 30 Dec 1965

AEDC-TR-65-4

MIXING AND BURNING OF BOUNDED COAXIAL STREAMS

C. E. Peters, T. Peters, and R. B. Billings

ARO, Inc.

March 1965

ROCKET TEST FACILITY
ARNOLD ENGINEERING DEVELOPMENT CENTER
AIR FORCE SYSTEMS COMMAND
ARNOLD AIR FORCE STATION, TENNESSEE

NOTICES

When U. S. Government drawings specifications, or other data are used for any purpose other than a definitely related Government procurement operation, the Government thereby incurs no responsibility nor any obligation whatsoever, and the fact that the Government may have formulated, furnished, or in any way supplied the said drawings, specifications, or other data, is not to be regarded by implication or otherwise, or in any manner licensing the holder or any other person or corporation, or conveying any rights or permission to manufacture, use, or sell any patented invention that may in any way be related thereto.

Qualified users may obtain copies of this report from the Defense Documentation Center.

References to named commercial products in this report are not to be considered in any sense as an endorsement of the product by the United States Air Force or the Government.

MIXING AND BURNING OF BOUNDED COAXIAL STREAMS

C. E. Peters, T. Peters, and R. B. Billings
ARO, Inc.

FOREWORD

The research presented was sponsored by Arnold Engineering Development Center (AEDC), AFSC, Arnold Air Force Station, Tennessee under Program Element 62405184, Project 6950, Task 695002.

The results of the research were obtained by ARO, Inc. (a subsidiary of Sverdrup and Parcel), contract operator of AEDC, under Contract AF40(600)-1000 and ARO Project No. RW2410. The report was submitted by the authors on December 18, 1964.

The cooperation and assistance of the Scientific Computing Branch is gratefully acknowledged. Mr. W. J. Phares, who assisted in the analysis and programmed the mixing theory for numerical solution with a high-speed digital computer, deserves special mention. Other members of the Scientific Computing Branch provided many helpful suggestions.

This technical report has been reviewed and is approved.

Eules L. Hively
Acting Chief, Propulsion Division
DCS/Research

Donald R. Eastman, Jr.
DCS/Research

ABSTRACT

An experimental and theoretical investigation of bounded turbulent mixing with chemical reactions is described. Configurations which are applicable to the air-augmented rocket are considered. Experimental results are presented for a mixing apparatus in which a fuel-rich O_2-H_2 rocket stream was mixed with a secondary air stream inside a conical duct. An integral mixing theory is described, in which conservation equations are satisfied across the duct. The inviscid portions of the duct flow are considered one-dimensional, and the mixing zone profiles are assumed to exhibit shape similarity. The theory is extended to include the downstream regime where the mixing region extends across the entire duct. Correlations of the theory with incompressible and reactive compressible mixing experiments indicate that the theory provides a satisfactory overall representation of the bounded mixing process.

CONTENTS

ILLUSTRATIONS

TABLE

NOMENCLATURE

A	Area
A_D	Duct area
b	Width of mixing zone
C	Element mass fraction
$\bar{C}$	Mass fraction of elements from central stream
c_f	Friction coefficient
D	Duct diameter
F_D	Mixing duct thrust
F_j	Rocket vacuum thrust
H	Static enthalpy, including chemical heats of formation
$\bar{H}$	Boundary-layer shape parameter, δ^*/θ
H_o	Stagnation enthalpy, including chemical heats of formation
h	Static enthalpy
h_o	Stagnation enthalpy
k_I, k_{II}	Turbulent spreading constants
k'	Constant in eddy viscosity equation
L	Duct length

M	Mach number
O/F	Rocket oxidizer-fuel mass ratio
p	Static pressure
p_o	Stagnation pressure
p'_o	Pitot pressure
Q	Species conservation parameter (defined by Eq. 10)
r	Radius
T_o	Stagnation temperature
u	Time average axial velocity
v	Time average radial velocity
w	Mass flow rate
x	Axial distance
γ	Ratio of specific heats
δ^*	Boundary-layer displacement thickness
ϵ	Turbulent eddy viscosity
θ	Boundary-layer momentum thickness
ρ	Density
τ	Turbulent shear stress

SUBSCRIPTS

1	Mixing duct inlet
2	Mixing duct exit
a	Outer inviscid stream (secondary)
c	Centerline
i	Inner boundary of mixing zone
j	Central inviscid stream (primary)
M	Duct half radius position
ne	Nozzle exit
w	Wall

SUPERSCRIPTS

*	Outer stream choking section

SECTION I
INTRODUCTION

There is currently considerable interest in air-augmentation as a method for significantly increasing the performance of fuel-rich chemical rockets during atmospheric flight. Of particular interest is the configuration shown in Fig. 1, which consists of a divergent mixing duct connected to an annular air inlet located near the missile base. The rocket exhaust and air streams mix and burn inside the duct, and a net increase in thrust is obtained if the axial pressure force on the mixing duct inner surface is larger than the combined inlet and external drag. The weight of the additional hardware must also be considered.

Divergent air-augmentation configurations were first investigated experimentally in 1950 (Ref. 1) for the case where the secondary stream stagnation pressure was equal to the ambient pressure at the duct exit (corresponding to zero flight velocity). More recently, divergent air-augmentation configurations have been proposed (Ref. 2) for use at high vehicle velocities with substantial ram compression of the secondary air. The performance of such air-augmented rockets has been analyzed by assuming complete mixing and burning (or some fraction thereof) with arbitrary pressure distributions along the mixing duct (Ref. 2). Although this type of one-dimensional analysis serves to point out the overall potential of the air-augmented rocket, it is incapable of predicting the duct shape required to realize an assumed pressure distribution, or of predicting the performance attainable with mixing ducts of practical shape. A perceptive theory for the complex process of bounded mixing and burning is required for realistic evaluation and optimization of the air-augmented rocket. The phenomenon of bounded mixing, with or without burning, is also encountered in other devices, for example, the supersonic combustion ramjet and the jet pump. For a jet pump with a constant area mixing duct, one-dimensional theory satisfactorily predicts the overall performance; however, the length of duct required to attain the performance predicted by one-dimensional theory can be predicted only by a detailed analysis of the mixing process.

This report summarizes the results of an experimental and theoretical investigation of the bounded coaxial stream mixing problem. The fundamental objective of this investigation is to determine (for a given central stream, duct configuration, and secondary stream stagnation pressure) the induced secondary flow and duct wall pressure distribution. Because of the very complex nature of this problem, many simplifications are required in a theoretical treatment of the overall duct flow. Use of integral conservation equations, however, provides overall results which are sufficiently accurate for engineering analysis, even though the detailed

mechanisms are over-simplified. Emphasis has been placed on relatively long mixing configurations in which the mixing region encompasses most or all of the duct cross section and in which the mixing cannot be considered a perturbation on the inviscid flow fields which would exist without mixing.

The bounded mixing problem can be divided into three distinct regimes as shown in Fig. 2. In the first regime, turbulent mixing occurs between the inviscid central and outer streams. In the second regime, the central inviscid stream has been dissipated, but a region of inviscid secondary flow exists near the duct wall. The third regime occurs when the mixing zone spreads to the wall. In the first two regimes, the mixing is essentially free turbulent in nature, although at variable pressure, and free turbulent spreading relations may be applied. The third regime, however, requires a departure from the techniques used in the analysis of free turbulent mixing.

The mixing zone chemistry is assumed to be either frozen or in equilibrium; that is, the chemistry is considered to be either very slow or very fast with respect to a characteristic time for the flow.

SECTION II
FORMULATION OF MIXING THEORY

Theoretical treatments of free turbulent mixing with chemical reactions are usually limited to constant pressure, or to the case of a prescribed axial pressure distribution (e.g., Refs. 3, 4). The presence of a wall in proximity to the mixing region, however, causes the axial pressure distribution to be strongly dependent upon the mixing process. The bounded mixing problem then involves simultaneous solution of the inviscid stream flow conditions along with the mixing zone conditions. The integral technique, in which overall conservation equations are satisfied across the mixing region, is used in this analysis. Use of the integral method is advantageous in that the overall results (i.e., wall pressure distribution) are relatively insensitive to the choice of mixing zone profiles. Similar techniques have been used by Mikhail (Ref. 5) and Yakovlevskiy (Ref. 6) for incompressible bounded mixing.

A useful relationship between the velocity, enthalpy, and composition distributions can be obtained by considering the conservation equations in differential form, with turbulent Prandtl and Lewis numbers of unity (Ref. 3):

Momentum equation:

$$\rho u \frac{\partial u}{\partial x} + \rho v \frac{\partial u}{\partial r} = r^{-1} \frac{\partial}{\partial r}\left(\rho \epsilon r \frac{\partial u}{\partial r}\right) - \frac{\partial p}{\partial x} \qquad (1)$$

Energy equation:

$$\rho u \frac{\partial H_o}{\partial x} + \rho v \frac{\partial H_o}{\partial r} = r^{-1} \frac{\partial}{\partial r}\left(\rho \epsilon r \frac{\partial H_o}{\partial r}\right) \tag{2}$$

Conservation of elemental species:

$$\rho u \frac{\partial C}{\partial x} + \rho v \frac{\partial C}{\partial r} = r^{-1} \frac{\partial}{\partial r}\left(\rho \epsilon r \frac{\partial C}{\partial r}\right) \tag{3}$$

Global continuity equation:

$$\frac{\partial}{\partial x}(\rho u) + r^{-1} \frac{\partial}{\partial r}(\rho \tilde{v} r) = 0 \tag{4}$$

These equations are the laminar boundary-layer equations with the laminar transport properties replaced by the corresponding effective turbulent values. Consider the case of constant pressure mixing of an initially uniform jet with a surrounding uniform infinite stream. The dp/dx term in Eq. (1) is then zero, and Eqs. (1), (2), and (3) are identical in form. A linear relation is obtained between the variables u, H_o, and C:

$$\frac{H_o - H_{oa}}{H_{oj} - H_{oa}} = \frac{C - C_a}{C_j - C_a} = \frac{u - u_a}{u_j - u_a} \tag{5}$$

The stagnation enthalpy, H_o, is defined to include the chemical heats of formation. For constant pressure mixing, H_o and C are related to velocity by Eq. (5), and solution of momentum and global continuity equations completely defines the flow field. For application to an integral method, Eq. (5) is also assumed to be valid for mixing with moderate axial pressure gradients. Note, however, that the inviscid stream reference velocities are now pressure dependent.

The additional assumptions made in the integral treatment for bounded mixing are as follows:

1. The inviscid streams are one-dimensional and isentropic.
2. The static pressure is constant across any duct section.
3. Wall viscous effects on the velocity profiles are neglected. However, for very long mixing ducts, the wall boundary-layer effect may be included as a wall displacement.
4. The velocity profile at the initiation of mixing is a step function.
5. If the central stream is supersonic and not correctly expanded, a one-dimensional isentropic adjustment process is assumed in which the central and outer streams expand or contract until pressure equilibrium is reached and the combined stream areas equal the initial duct area.

2.1 FIRST REGIME

The integral conservation equations in axisymmetric coordinates (Fig. 3) are:

Axial momentum across the duct:

$$\frac{\partial}{\partial x}\int_0^{r_w} \rho u^2\, r\,dr = -\frac{\partial p}{\partial x}\int_0^{r_w} r\,dr \tag{6}$$

Steady flow continuity:

$$\frac{\partial}{\partial x}\int_0^{r_w} \rho u\, r\,dr = 0 \tag{7}$$

These equations become for the three regions of the flow (central inviscid stream, mixing zone, and outer inviscid stream):

$$\frac{\partial}{\partial x}\left\{\rho_j u_j^2 \frac{r_i^2}{2} + \rho_a u_a^2 \left[\frac{r_w^2-(r_i+b)^2}{2}\right] + \int_{r_i}^{r_i+b} \rho u^2\, r\,dr\right\} = -\frac{\partial p}{\partial x}\frac{r_w^2}{2} \tag{6a}$$

$$\frac{\partial}{\partial x}\left\{\rho_j u_j \frac{r_i^2}{2} + \rho_a u_a \left[\frac{r_w^2-(r_i+b)^2}{2}\right] + \int_{r_i}^{r_i+b} \rho u\, r\,dr\right\} = 0 \tag{7a}$$

The inviscid stream densities and velocities (ρ_a, ρ_j, u_a, u_j) are isentropic functions only of p.

2.1.1 Mixing Zone Profiles

For free mixing with moderate axial pressure gradients, it is well established that experimental mixing zone velocity profiles exhibit shape similarity at various axial stations:

$$\frac{u-u_a}{u_j-u_a} = f\left(\frac{r-r_i}{b}\right)$$

Various profile shape equations are available which correlate reasonably well with experimental velocity distributions. The integral method is not sensitive to the profile chosen so long as it is a reasonable representation of the experimental shape. A cosine profile was used because this profile reaches the inviscid stream velocities at finite radial distances,

$$\frac{u-u_a}{u_j-u_a} = \frac{1}{2}\left[1+\cos\pi\left(\frac{r-r_i}{b}\right)\right] \tag{8}$$

For frozen mixing, Eq. (5) may be interpreted as

$$\frac{h_o-h_{oa}}{h_{oj}-h_{oa}} = \frac{C-C_a}{C_j-C_a} = \frac{u-u_a}{u_j-u_a} \tag{5a}$$

where h_o is the sensible enthalpy. Because there is no chemical reaction, C may be taken as the mass fraction of any specie. The mixing zone specific heat and gas constant are evaluated as mass averages of the constituent values.

For mixing with chemical reactions, Eq. (5) is defined as

$$\frac{H_o - H_{oa}}{H_{oj} - H_{oa}} = \frac{u - u_a}{u_j - u_a} = \frac{\bar{C} - \bar{C}_a}{\bar{C}_j - \bar{C}_a} = \bar{C} \tag{5b}$$

where $\bar{C}$ is the mass fraction of elements originating in the central stream (thus $\bar{C}_a = 0$ and $\bar{C}_j = 1$). This composition parameter is convenient when the inviscid streams consist of several elemental species. The assumption of equilibrium mixing zone chemistry, along with the energy equation and the perfect gas law, then gives the mixing zone temperature and density for any velocity. This treatment of the mixing zone implies that, at any point on the non-dimensional profile, the mass fractions of the elements are the same as for frozen mixing and that chemical reaction shifts only the local temperature and gas properties from the frozen values.

To simplify the computation procedure for the equilibrium chemistry case, temperature and gas property functions of $\bar{C}$ were computed at representative values of p, u_j, and u_a, using the method presented in Appendix I. The distribution of total temperature was then computed, and the gas property and total temperature functions of $\bar{C}$ were taken as constant throughout a computation. By using this technique, the chemistry enters the mixing problem only through the gas property and total temperature functions of $\bar{C}$; a typical set of these functions is shown in Figs. 4, 5, and 6.

2.1.2 Turbulent Spreading Rate

The mixing zone profiles of ρ and u are now known with respect to dimensionless position in the mixing zone. A relation expressing the rate of growth, db/dx, of the mixing zone, is required to allow solution of Eqs. (6a) and (7a) for p(x) and $r_i(x)$. Abramovich (Ref. 7) proposed the following relationship for free turbulent mixing with large density gradients:

$$\frac{db}{dx} = \frac{k_I}{2} \frac{(\rho_j u_j^2 - \rho_a u_a^2) \int_0^1 \rho \, d\left(\frac{r - r_i}{b}\right)}{\left[\int_0^1 \rho u \, d\left(\frac{r - r_i}{b}\right)\right]^2} \tag{9}$$

where k_I is one-half the incompressible mixing zone spreading rate for $u_a = 0$. The value for k_I is established as about 0.13 (Ref. 8); however, the experimental determination of k_I from mixing zone velocity measurements is very difficult because the outer edges of the mixing zone are not easily located. It is also probable that the analytical velocity profile used in a particular theory is not an exact representation near the

low velocity boundary; therefore, a better procedure for determining k_I is to correlate the particular theory with incompressible experiments to give the best overall representation of the flow.

2.1.3 Elemental Species Conservation

The relation between mixing zone velocity and concentration (Eq. 5) was deduced from the conservation equations for the case of constant pressure mixing. The same relation was assumed to be valid for variable pressure mixing, and the validity of this assumption is checked throughout the mixing theory computations. Continuity of the central stream elemental species is checked by evaluating the function,

$$Q = \frac{2\pi}{w_j} \int_0^{r_w} \rho u \bar{C} \, r dr \tag{10}$$

If Q does not deviate from unity, then elemental species continuity is satisfied, and use of Eq. (5) is justified, at least for use in an integral method.

2.2 SECOND REGIME

The second regime is treated in the same manner as the first, except that the mixing zone orientation, r_j, is replaced as a variable by the centerline velocity, u_c. Equations (6) and (7) become

$$\frac{\partial}{\partial x}\left[\rho_a u_a^2 \frac{r_w^2 - b^2}{2} + \int_0^b \rho u^2 \, r dr\right] = -\frac{\partial p}{\partial x}\frac{r_w^2}{2} \tag{6b}$$

and

$$\frac{\partial}{\partial x}\left[\rho_a u_a \frac{r_w^2 - b^2}{2} + \int_0^b \rho u \, r dr\right] = 0 \tag{7b}$$

The profile shape equation becomes

$$\frac{u - u_a}{u_c - u_a} = \frac{1}{2}\left[1 + \cos \pi \left(\frac{r}{b}\right)\right] \tag{8a}$$

The turbulent spreading rate equation becomes

$$\frac{db}{dx} = \frac{k_{II}}{2} \frac{(\rho_c u_c^2 - \rho_a u_a^2) \int_0^1 \rho \, d\left(\frac{r}{b}\right)}{\left[\int_0^1 \rho u \, d\left(\frac{r}{b}\right)\right]^2} \tag{9a}$$

The value of the second regime spreading parameter is reported as 0.11 (Ref. 8), but again, it should be evaluated by correlating the theory with incompressible experiments.

2.3 THIRD REGIME

Mikhail (Ref. 5) and Yakovlevskiy (Ref. 6) have shown that, for incompressible flow, the velocity profiles in the third regime have essentially the same shape as free mixing profiles. Of course, very far downstream the wall effects predominate, and the profile loses the free mixing shape; however, for a few diameters downstream, the wall shear is small compared to the free turbulent shear, and the assumption of profile shape similarity is justified. The concept of mixing zone growth rate is no longer valid in the third regime; therefore, the turbulent spreading relation is replaced by an additional momentum equation written from the centerline to the duct half radius (Fig. 7):

$$\frac{\partial}{\partial x}\int_0^{r_w/2} \rho u^2 \, r\,dr - u_M \frac{\partial}{\partial x}\int_0^{r_w/2} \rho u \, r\,dr = -\tau_M \frac{r_w}{2} - \frac{\partial p}{\partial x}\int_0^{r_w/2} r\,dr \qquad (11)$$

where the subscript M refers to the duct half radius position. For a considerable distance downstream, the turbulent shear at the profile midpoint will be free turbulent in nature, and may be expressed as

$$\tau_M = \rho_M \epsilon \left.\frac{\partial u}{\partial r}\right|_M \qquad (12)$$

where ϵ is the free turbulent eddy viscosity. The Prandtl formulation for ϵ is

$$\epsilon = k' b \, (u_{max} - u_{min}) \qquad (13)$$

where ϵ is assumed constant across the mixing zone. It is well known that ϵ is not constant laterally for incompressible flow and is certainly not for mixing with large density gradients. The procedure used in this study was to assume that Eq. (13) is functionally valid along the velocity profile midpoint and may be used to extrapolate the half radius shear stress, $\bar{\tau}_M$, which is evaluated by solving Eq. (11) at the end of the second regime. The half-radius shear stress is then at any station, replacing b by r_w,

$$\tau_M \propto \rho_M \, (u_c - u_w)^2$$

and the relation used to relate τ_M to $\bar{\tau}_M$ is

$$\tau_M = \bar{\tau}_M \frac{\rho_M \, (u_c - u_w)^2}{\bar{\rho}_M \, (\bar{u}_c - \bar{u}_w)^2} \qquad (14)$$

where the barred variables are those evaluated at the end of the second regime.

The three conservation equations (6), (7), and (11) may now be solved for the unknowns, u_c, u_w, and p. The integral conservation equations have been transformed to a form suitable for numerical computations (Ref. 9) and are solved with a high-speed digital computer.

SECTION III
EXPERIMENTAL PROGRAM

The RTF Propulsion Research Cell (R-1B) (Fig. 8) was designed to investigate the bounded mixing and burning process. A small scale rocket was used to provide the primary stream, and atmospheric air was used for the secondary stream. A conical mixing duct was used. The cell was connected to the RTF exhauster system, which maintained the back pressure on the mixing duct at approximately 2.5 psia. The principal dimensions and operating parameters for the apparatus are given in Table I.

In addition to the usual measurements of rocket and air stream parameters, the following parameters were measured:

1. Mixing duct static pressure distribution,
2. Pitot pressure distribution across mixing duct exit plane, and
3. Gas composition distribution across mixing duct exit plane.

3.1 ROCKET ENGINE

A water-cooled, oxygen-hydrogen rocket engine was used to generate a high temperature stream of fuel-rich exhaust gases. The characteristic length, L* (chamber volume/throat area), of the rocket chamber was approximately 35 in.

The oxygen-hydrogen propellant combination was chosen because of the relatively simple exhaust gas composition which lends itself readily to gas analysis. Gaseous propellants were chosen to achieve a high combustion efficiency; liquid-propellant rocket engines of this scale normally operate at much lower combustion efficiency than a comparable large booster engine. A rocket engine having high combustion efficiency is necessary for accurate experimental evaluation of rocket thrust augmentation configurations in which afterburning of the rocket exhaust occurs. If the rocket is inefficient, an unrealistically large amount of unburned fuel is available for afterburning. This excessive afterburning can lead to erroneous conclusions about the performance of the augmented rocket as compared to that of the basic rocket.

The theoretical combustion temperature of the gaseous O_2-H_2 engine is approximately 5300°R. The characteristic velocity, c^* (defined as chamber pressure times throat area divided by propellant flow), is

normally used as a measure of combustion efficiency. For the 25 firings discussed in this report, the experimental value of c* averaged 97 percent of theoretical c*. Most of the deviation from ideal c* results from heat transfer to the cooling water.

3.2 INSTRUMENTATION

3.2.1 Wall Static Pressure

Wall static pressures throughout the apparatus were measured with mercury manometers, referenced to atmosphere and recorded photographically. Mixing duct static pressures were measured with two rows of taps 90 deg apart; the axial tap spacing was 2 in.

A vacuum check was made prior to and following each test to detect any leaks in the manometer system. The scales on the manometers were subdivided into 0.1-in. increments, and the resulting pressures were read with an estimated precision of ±0.05 psi.

3.2.2 Air Flow Rate

The secondary airflow was measured with a choked venturi, having a circular arc inlet contour and a conical diffusion section. For the range of throat Reynolds number encountered, the nozzle flow coefficient was greater than 0.99 (Ref. 10); therefore the coefficient was assumed to be unity. The stagnation pressure of the venturi flow was measured with mercury manometers, and the stagnation temperature was measured with an immersion-type thermocouple.

3.2.3 Propellant Flow Rates

The propellant flows were also measured with choked venturis. Propellant temperatures were measured with immersion-type thermocouples which were located downstream from the venturis to avoid distorting the inlet flow. The nozzle flow coefficients were again, for the range of throat Reynolds number encountered, greater than 0.99 (Ref. 10).

3.2.4 Rocket System Pressures

Rocket chamber pressure and the propellant metering nozzle inlet pressures were measured with strain-gage-type transducers and recorded on direct-inking, null-balance potentiometers. The systems were periodically calibrated against a secondary standard to check for non-linearity and for absolute level. The calibrations were checked prior to each test period by applying a fixed resistance to the system to obtain a full-scale deflection.

During shakedown of the apparatus, the propellant pressures downstream from the metering nozzles were measured with similar instrumentation. These pressure measurements were discontinued after it was found that the pressure drops across the venturis were sufficient to ensure choked flow at the nozzle throats.

3.2.5 Temperatures

Air stream temperature was measured with an immersion-type thermocouple and recorded on a multi-point, null-balance potentiometer.

The propellant temperatures were measured with immersion-type thermocouples and recorded on a light-beam oscillograph. The thermocouple system was calibrated by applying known voltage from a standard cell and recording the galvanometer deflection. The thermocouples were referenced to control room temperature which was measured with a mercury bulb thermometer.

3.2.6 Survey Rake

The mixing duct exit plane surveys were made with a water-cooled, thirteen-probe rake having seven pitot pressure probes and six gas sampling probes (Fig. 9). The rake was installed with the probe tips about 1/4 in. downstream from the mixing duct exit; a complete survey of the exit plane flow was accomplished by installing the rake during different tests with various spacers at the rake mounting flange. Details of the probe tip construction are shown in Fig. 9b.

The gas sampling probes were similar to those used by Rhodes, et al (Ref. 11) in their investigations of shock-induced combustion of hydrogen-air mixtures. A sapphire watch bearing (fused aluminum-oxide) was imbedded in the probe tip to provide an orifice capable of withstanding the high stream temperatures. The probe was designed so that the expansion of the sample flow inside the probe, and the subsequent cooling effect of the inner probe walls, would cause quenching of the major chemical reactions. The gas samples were taken in evacuated bottles and were later analyzed for N_2, O_2, and H_2 with a gas chromatograph.

The rake pitot pressures were measured with mercury manometers referenced to atmosphere. Near the duct centerline, however, the pressures were too high to be measured with the available 100-in. manometers, and dial-type bourdon-tube gages were used. These gages were graduated in 0.2-psi increments and could be read with an estimated precision of ±0.1 psi.

3.3 EXPERIMENTAL PROCEDURE

The desired airflow was set by adjusting a throttle valve upstream of the venturi. The rocket was then fired for a nominal duration of 30 sec. Photographs of the manometer boards were taken after stabilization. Gas samples were taken during a 20-sec period following rocket stabilization.

SECTION IV
RESULTS AND DISCUSSION

4.1 INCOMPRESSIBLE BOUNDED MIXING

The mixing theory has been correlated with the low velocity jet pump experiment of Mikhail (Ref. 5) to evaluate the theory for incompressible flow and to determine the incompressible values for the turbulent spreading parameters. Mikhail's apparatus is shown in Fig. 10, along with the principal experimental parameters. The experimental axial duct pressure distribution is shown in Fig. 11. Theoretical pressure distributions are also shown for two cases: (1) wall boundary-layer effect neglected and (2) wall boundary-layer effect considered as an estimated linear displacement thickness. Both theoretical curves were computed with $k_I = k_{II} = 0.11$ (compared to 0.13 and 0.11 reported in Ref. 8 for free mixing). The theory predicts the inflected pressure distribution, which is characteristic for the low velocity jet pump. Theoretical and experimental axial distributions of centerline velocity are shown in Fig. 12. The theoretical distribution agrees well with the experiment in the first and second mixing regimes, and the agreement is satisfactory for about three duct diameters downstream into the third regime. Further downstream, the theory does not predict as much centerline velocity decay as was observed experimentally. This indicates that the flow is no longer free turbulent in nature but that the wall effects are beginning to predominate.

4.2 O_2-H_2 ROCKET EXPERIMENTS

For the experiments which have been conducted during this investigation, the non-one-dimensional effects in the jet plume from the conical rocket nozzle cannot be neglected when applying the mixing theory. The rocket exhaust jet expands from the nozzle and causes the outer air stream to choke at some distance, x^*, downstream from the initial section

(Fig. 13a). The outer stream is supersonic downstream from the choking section. Because the plume is not one-dimensional, the jet cross-sectional area is larger than if the expansion were actually one-dimensional. The secondary flow is directly proportional to the secondary stream choking area, A_a^*, and the following procedure was used to determine that area. First, the streams are assumed to be inviscid up to the choking station, and the plume shape is assumed to be adequately represented by a plume issuing from the rocket into an ambient medium at p_a^*. The resulting plume area distribution, as computed by the method of characteristics, along with the duct area distribution, gives a distribution of outer stream area. The minimum area is taken to be A_a^*, and the area distribution up to the choke point defines the outer stream pressure distribution.

The mixing theory is patched onto the inviscid plume analysis at the choke point, and the difference between the plume cross-sectional area and one-dimensional area is treated as a small parallel wall shift (Fig. 13b). This approximate treatment of the non-uniform central jet flow must be regarded as tentative and is inadequate for a treatment of the flow where L is approximately equal to x^*. For long mixing ducts, where L is much larger than x^*, the downstream flow is relatively insensitive to the non-uniform initial conditions, and the approximate treatment is sufficiently accurate for engineering analysis.

The induced air-rocket mass ratio, w_a/w_j, for the O_2-H_2 rocket configuration is shown in Fig. 14, plotted against the stagnation pressure ratio, p_{oa}/p_{oj}. The theoretical curve, calculated with the inviscid plume analysis, is generally higher than the experimental points, with less than 5 percent deviation over most of the experimental range of p_{oa}/p_{oj}.

Typical experimental mixing duct static pressure distributions are shown in Figs. 15a and b for w_a/w_j of 5.3 and 3.6, respectively. The theoretical pressure distributions were calculated up to x^* by the inviscid plume analysis, and downstream of x^* by the mixing theory with the assumption of equilibrium mixing zone chemistry and $k_f = 0.10$. The theory predicts that a small core of the inviscid rocket stream exists at the duct exit; therefore, only the first mixing regime is encountered with this configuration. The experimental pressure distribution reflects the tendency of the jet to alternately expand and contract because of the non-one-dimensional effects; the theory represents an averaged downstream distribution.

The results of a pitot pressure survey across the mixing duct exit plane are shown in Figs. 16a and b for the same experimental conditions as for the wall pressure distributions in Figs. 15a and b. The experimental points represent the results of several tests at each operating condition. The experimental distributions were plotted radially from the

centerline of the profiles, which was displaced about 1/4 in. from the duct centerline. The symmetry of the experimental profiles can be seen by noting that the flagged symbols, which represent measurements on the opposite side of the duct, generally fall along the same distribution as the unflagged symbols. The theoretical distribution in Fig. 16a is seen to agree satisfactorily with the experimental distribution; however, the experimental points near the profile centerline in Fig. 16b fall considerably below the theory. It is probable that this deviation results from substantially larger stagnation pressure losses in the inviscid rocket stream for the low secondary pressure case as compared to the higher pressure case. For the lower pressure, the rocket stream initially plumes to a greater extent, and consequently, the downstream shock system in the inviscid jet is stronger. It is assumed in the theory that these inviscid stream losses are negligible.

The results of exit plane gas composition surveys are shown in Figs. 17a and b for the same experimental conditions as for the data shown in Figs. 15 and 16. The radial distributions of N_2, O_2, and H_2 agree reasonably well with those predicted by the theory, with the assumption of equilibrium mixing zone chemistry. The experimental points shown represent the results of several tests at each operating condition. As with the pitot pressure data, the flagged symbols represent samples taken on the side of the profile centerline opposite to that for the unflagged symbols.

The thrust performance of this mixing duct configuration is shown in Fig. 18, plotted as the duct thrust integral, $F_D = \int^{2} p\,dA$, divided by the theoretical rocket vacuum thrust, F_j. The experimental values of F_D were obtained by graphical integration of the duct pressure distributions. The duct thrust predicted by the mixing theory with the initial plume analysis is seen to agree with the experimental results to within a few percent over the experimental range of secondary stream stagnation pressure. The flagged symbols in Fig. 18, which fall consistently below the other points, represent thrust results obtained during one testing period, and their validity is subject to question. Careful examination of all the experimental parameters measured during that testing period, however, failed to yield a definite reason for the experimental deviation. It is possible that the reference pressure for the manometers on which the duct static pressures were measured was slightly different from atmospheric because of an obstruction in a line.

The central stream species parameter, Q, did not vary more than one percent from unity in any of the theoretical computations for this configuration.

Various values of k_I were used to correlate the theory with these experiments. The best overall correlation was obtained with $k_I = 0.10$,

as compared with $k_I = 0.11$ used to correlate the incompressible experiments. If the Abramovich turbulent spreading relation were exact, the value of kI should also have been 0.11 for the O_2-H_2 experiments. The Abramovich relation is thus not exact but predicts a slightly excessive rate of mixing for the case of very large density gradients in the mixing zone.

The mixing zone chemistry appears to be nearly in equilibrium for these experimental conditions, based on the overall correlation between theory and experiment. The mixing duct static pressure distributions, and radial exit plane distributions of composition and pitot pressure, are satisfactorily predicted with the assumption of equilibrium chemistry incorporated in the mixing theory.

4.3 EFFECT OF PRESSURE GRADIENTS

The turbulent spreading rate, db/dx, calculated from Eq. 9 does not account for the effects of axial pressure gradients. It is well known that the rate of growth of a turbulent wall boundary layer is appreciably affected by axial pressure gradients, with negative pressure gradients tending to decrease the rate of growth. By analogy to the wall boundary layer, an expression was derived which shows that even small axial pressure gradients can significantly influence the turbulent spreading rate when the width of the mixing zone is large. By writing the momentum integral equation for a wall boundary layer, with the inviscid stream denoted by the subscript ∞,

$$\frac{d\theta}{dx} = \frac{c_{fw}}{2} + \frac{\bar{H} + 2}{\rho_\infty u_\infty^2}\,\theta\,\frac{dp}{dx}$$

where θ is the momentum thickness and $\bar{H}$ the shape parameter. If this equation is applied to the free turbulent layer, with the central inviscid stream as the reference stream, then

$$\frac{d\theta}{dx} = \frac{c_f}{2} + \left(\frac{\theta}{b}\right)\frac{\bar{H} + 2}{\rho_j u_j^2}\,b\,\frac{dp}{dx}$$

The free turbulent friction coefficient, c_f, is a function of the local flow conditions and not of dp/dx; therefore, the rate of growth of the turbulent zone can be significantly different from the constant pressure rate only if the quantity $\left[\left(\frac{\theta}{b}\right)\frac{\bar{H} + 2}{\rho_j u_j^2}\,b\,\frac{dp}{dx}\right]$ is significant with respect to $c_f/2$, which can occur if either b or dp/dx is large. If the constant pressure spreading rate is denoted by the subscript o, then

$$\frac{db}{dx} = \frac{db}{dx}\bigg|_o \frac{\left[\frac{c_f}{2} + \left(\frac{\theta}{b}\right)\frac{\bar{H} + 2}{\rho_j u_j^2}\,b\,\frac{dp}{dx}\right]}{\frac{c_f}{2}}$$

or

$$\frac{db}{dx} = \frac{db}{dx}\bigg|_o \left[1 + 2\left(\frac{\theta}{b}\right)\frac{(\bar{H} + 2)}{c_f\,\rho_j\,u_j^2}\,b\,\frac{dp}{dx}\right] \tag{15}$$

If Eq. (15) is applied to the high velocity half of the mixing zone, the midpoint friction coefficient, c_{f_M}, is used. The shape parameter, $\bar{H}$, and momentum thickness, θ, are evaluated for the high velocity half of the layer. These quantitues were computed for a mixing region typical for the O_2-H_2 rocket configuration, and the quantity $\left[.2\left(\frac{\theta}{b}\right)\frac{\bar{H}+2}{c_{f_M}}\right]$ was found to be about 10. For the pressure gradients encountered in the O_2-H_2 rocket experiments, the value of db/dx was only slightly different from $db/dx|_o$, and the pressure gradient effect was neglected. The pressure gradient effect was also neglected in the incompressible jet pump correlations. This tentative analysis does point out, however, that Eq. (9) can be considerably in error for mixing configurations which have large axial pressure gradients or large mixing zone widths. A more rigorous treatment of the pressure gradient effect on mixing rates would be required to treat such configurations.

SECTION V
CONCLUSIONS

The following conclusions can be drawn from the results of this investigation of bounded turbulent mixing with chemical reaction:

1. The integral mixing theory provides a satisfactory overall representation of the bounded turbulent mixing process.
2. The assumption that the elemental species concentration is linearly related to the mixing zone velocity appears to intrinsically satisfy the requirement of elemental species conservation.
3. The Abramovich turbulent spreading relation gives results which are approximately correct. The mixing rates for a very low density rocket stream are satisfactorily predicted, considering the current state of knowledge on turbulent mixing.
4. Correlation of theoretical and experimental results for the O_2-H_2 rocket configuration indicate that the mixing zone reactions are nearly in equilibrium at the mixing duct exit.

Further investigation is required on the following problems associated with bounded turbulent mixing: (1) the effect of pressure gradients on turbulent spreading rates, and (2) the effect of non-uniformities in the inviscid streams on the overall duct flow.

APPENDIX I
EQUILIBRIUM MIXING ZONE CHEMISTRY

The mixing zone composition (elements) varies between the composition of the unmixed central stream and the composition of the outer air stream; thus, the elemental fuel-oxidizer mass ratio varies with position across the mixing zone. The nitrogen-oxygen mass ratio also varies with position in the mixing zone because the nitrogen-oxygen elemental mass ratio in the central stream is generally different from that for air. Rather than compute the equilibrium mixing zone temperatures and gas properties with the usual cumbersome equilibrium chemistry calculation procedure, a technique has been developed, in which the tabulated equilibrium properties for fuel-air mixtures (e.g., Refs. 12 and 13) can be used to calculate the equilibrium properties of the mixing zone gases which have variable nitrogen-oxygen mass ratio.

NOMENCLATURE

The nomenclature used in this appendix is as follows:

c_p	Specific heat
g_c	Conversion constant
h	Static enthalpy of reactants (per unit mass)
J	Joule's constant
MW	Mixture molecular weight
m_i	Mass fraction of the i^{th} species
n_i	Mole fraction of the i^{th} species in reactants
N_i	Mole fraction of the i^{th} species in products
p	Static pressure of mixture
R	Mixture gas constant
T	Static temperature
T_o	Stagnation temperature
u	Local flow velocity

Unbarred symbols refer to the mixing zone system having a given fuel-oxygen mass ratio and having a given nitrogen-oxygen mass ratio.

Barred symbols refer to the equivalent fuel-air mixture having the nitrogen-oxygen mass ratio of air.

PROCEDURE

The General Electric tables for combustion gases (Refs. 12 and 13 for hydrogen and hydrocarbon fuels, respectively) contain the following parameters tabulated against T, for various values of static pressure, p, and fuel-air equivalence ratio:

1. $\bar{h}$ – Enthalpy of the reactants
2. $\overline{MW}$ – Molecular weight of products
3. $\bar{N}_{H_2}, \bar{N}_{O_2}$ – Mole fractions of products

Consider one mole of products of the equivalent fuel-air mixture at a given equivalence ratio. At any temperature, T, and static pressure, p, the equivalent fuel-air system is completely defined. If the nitrogen is assumed to be inert, then the only effect of the nitrogen on the equilibrium chemistry of the reacting species is in the relationship of the species partial pressures to the mixture pressure.

In the fuel-air system

$$\left(\overline{n_{N_2}/n_{O_2}}\right) = 3.76$$

In the variable nitrogen system, the nitrogen-oxygen ratio is determined from the mixing profiles as a mass ratio, m_{N_2}/m_{O_2}, and

$$n_{N_2}/n_{O_2} = 1.142 \; m_{N_2}/m_{O_2}$$

By considering one mole of fuel-air products, a certain fraction of the nitrogen must be removed to convert to the variable nitrogen system.

$$\Delta N_{N_2} = \bar{N}_{N_2} - N_{N_2} = \bar{N}_{N_2}\left(1 - \frac{n_{N_2}/n_{O_2}}{3.76}\right) \tag{I-1}$$

where $\bar{N}_{N_2}$ is the nitrogen mole fraction in the fuel-air products. The resulting number of moles is $(1 - \Delta N_{N_2})$, and the mass removed is $28.016\ \Delta N_{N_2}$. The molecular weight in the mixture is then

$$MW = \frac{\overline{MW} - 28.016\ \Delta N_{N_2}}{1 - \Delta N_{N_2}} \tag{I-2}$$

The resulting mixture pressure is

$$p = \bar{p}\ (1 - \Delta N_{N_2}) \tag{I-3}$$

The enthalpy of the reactants in the variable nitrogen system is

$$h = \frac{\overline{MW}\ \bar{h} - (28.016\ \Delta N_{N_2})\ h_{N_2}}{\overline{MW} - 28.016\ \Delta N_{N_2}} \tag{I-4}$$

where

h_{N_2} is determined at T.

The mole fractions of the products (except nitrogen) are

$$N_i = \frac{\bar{N}_i}{(1 - \Delta N_{N_2})} \tag{I-5}$$

The mole fraction of nitrogen in the products is

$$N_{N_2} = \frac{(\bar{N}_{N_2} - \Delta N_{N_2})}{(1 - \Delta N_{N_2})} \tag{I-6}$$

The calculation procedure used to determine the mixture temperature, gas properties, and composition of an equilibrium system with mixture pressure, p, and reactant enthalpy, h, is as follows:

1. Assume an equivalent system pressure, $\bar{p}$.
2. Guess the static temperature of the products, T.
3. Calculate ΔN_{N_2}, MW, p, h, and product mole fractions from Eqs. (I-1) through (I-6).
4. Repeat steps (2) and (3) until the calculated value of h equals the initial value, thus defining T.
5. Repeat steps (1) to (4) until the calculated value of p equals the initial value. The results vary slowly with p; therefore, a satisfactory procedure is to choose values of p so that the calculated values of p bracket the initial value. The results for h, $\overline{MW}$, and mole fractions are then obtained by interpolation.

MIXTURE PROPERTIES

The mixture specific heat is evaluated on a mass basis as

$$c_p = \Sigma\, m_i c_{p_i}$$

The mixture gas constant, on a mass basis, is

$$R = \frac{1545}{MW} \quad BTU/lb_m{}^\circ R$$

The mixture, γ, is given by

$$\gamma = \frac{c_p}{c_p - R}$$

For a given local flow velocity, u, the local stagnation temperature, T_o, is evaluated from energy equation:

$$T_o = T + \frac{u^2}{2\, c_p\, g_c\, J}$$

REFERENCES

1. Pool, H. L. and Charyk, J. V. "Theoretical and Experimental Investigations of the Mixing of a Supersonic Stream with an Induced Secondary Stream as Applied to Ducted Propulsive Devices." Project Squid Technical Report No. 25, Princeton University, September 1950.

2. Perini, R. L., Walker, R. E., and Dugger, G. L. "Preliminary Study of Air Augmentation of Rocket Thrust." Applied Physics Laboratory Report TG 545, January 1964.

3. Libby, P. A. "A Theoretical Analysis of the Turbulent Mixing of Reactive Gases with Application to the Supersonic Combustion of Hydrogen." General Applied Science Laboratories Technical Report No. 242, June 1961.

4. Vasiliu, J. "Determination of Temperature, Velocity, and Concentration Profiles in the Mixing Layer Between a Rocket Exhaust Jet and the Surrounding Supersonic Air Stream." Convair-Astronautics Report ERR-AN-005, March 1960.

5. Mikhail, S. "Mixing of Coaxial Streams Inside Closed Conduit." Journal of Mechanical Engineering Science, Vol. 2, No. 1, March 1960, pp 59-68.

6. Yakovlevskiy, O. V. "The Mixing of Jets in a Channel with Variable Cross Section." Izvestiya Akademii NaukSSSR, OTN, Mekhanika i Mashinostroyeniye, No. 1, 1962, pp 66-72 (English translation FTD-TT-62-1571).

7. Abramovich, G. N. "Mixing Turbulent Jets of Different Density." Izvestiya Akademii Nauk SSSR, Otdeleniye Tekhnicheskikh Nauk, Mekhanika i Mashinostroyeniye, No. 3, 1961, pp 55-57. (English translation FTD-TT-63-222).

8. Abramovich, G. N. "Turbulent Jets Theory." Gosudarstvennoye Izdatel' stvo Fiziko - Matematicheskoy Leteratury, Moscow, 1960. (English translation - WP-AFB Tech. Documents Liaison Office MCL-1256/1+2).

9. Phares, W. J. and Loper, F. C. "A Technique for Solving Integro-Differential Equations with Application to Turbulent Mixing." AEDC-TDR-64-209, November 1964.

10. Smith, R. E., Jr., and Matz, R. J. "Verification of a Theoretical Method of Determining Discharge Coefficients for Venturis Operating at Critical Flow Conditions." AEDC-TR-61-8 (AD263714), September 1961.

11. Rhodes, R. P., Rubins, P. M., and Chriss, D. E. "The Effect of Heat Release on the Flow Parameters in Shock-Induced Combustion." AEDC-TDR-62-78 (AD275366), May 1962.

12. Browne, W. G. and Warlick, D. L. "Properties of Combustion Gases - System H_2-Air." General Electric Co., Cincinnati, Ohio, R62FPD-366, November 1962.

13. H. A. Fremont, et al. "Properties of Combustion Gases - System C_nH_{2n} - Air." General Electric Co., Cincinnati, Ohio, 1955, (2 Volumes).

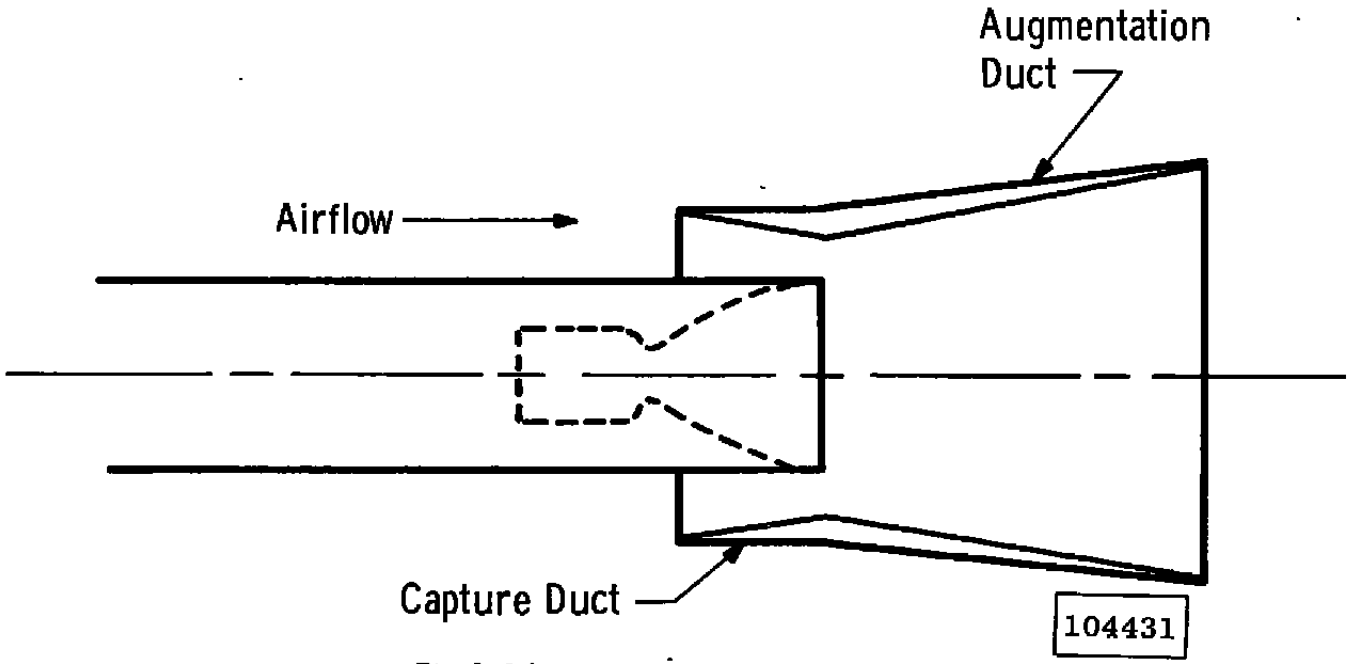

Fig. 1 Schematic of Air-Augemented Rocket

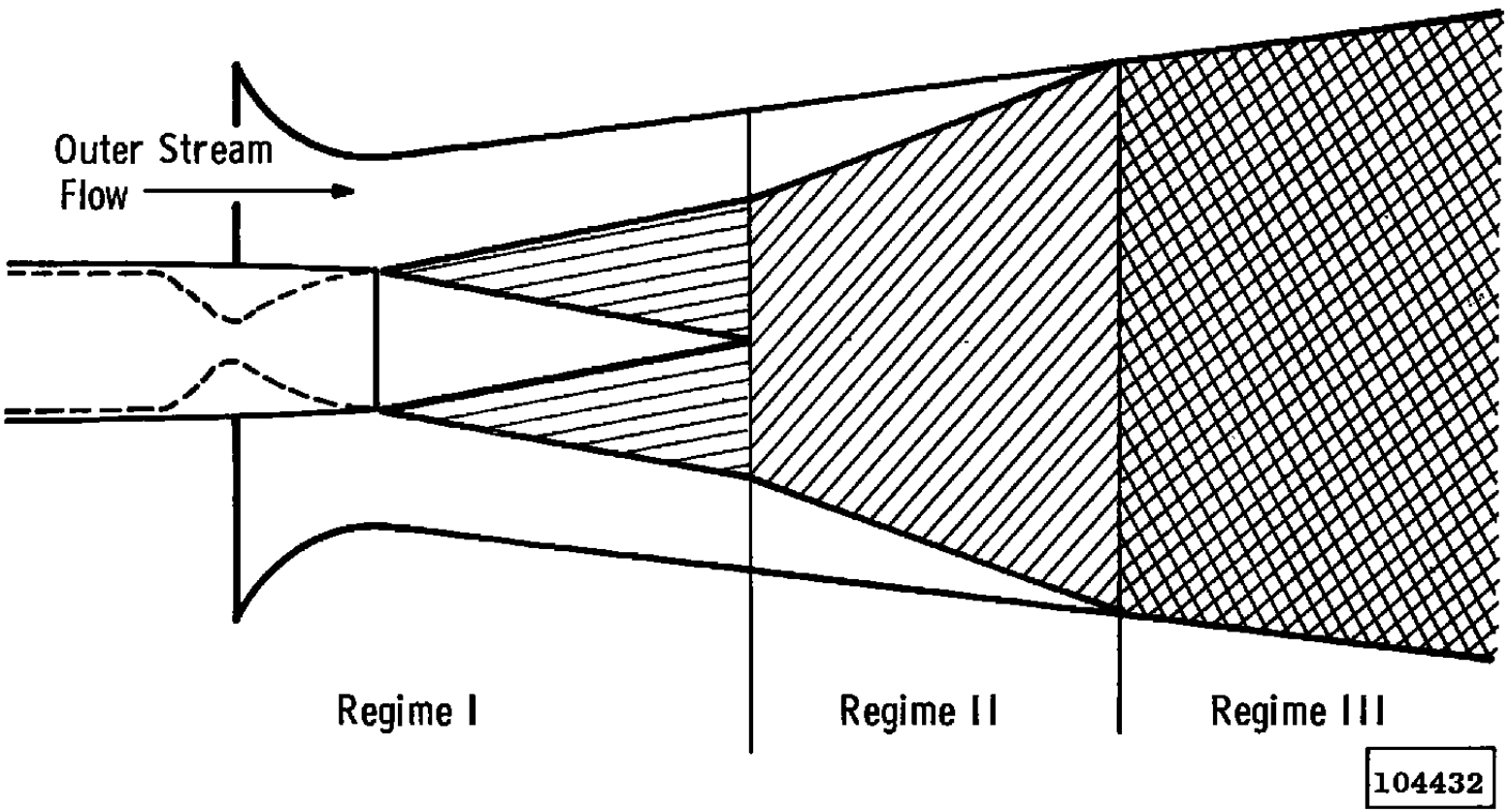

Fig. 2 Schematic of Duct Flow

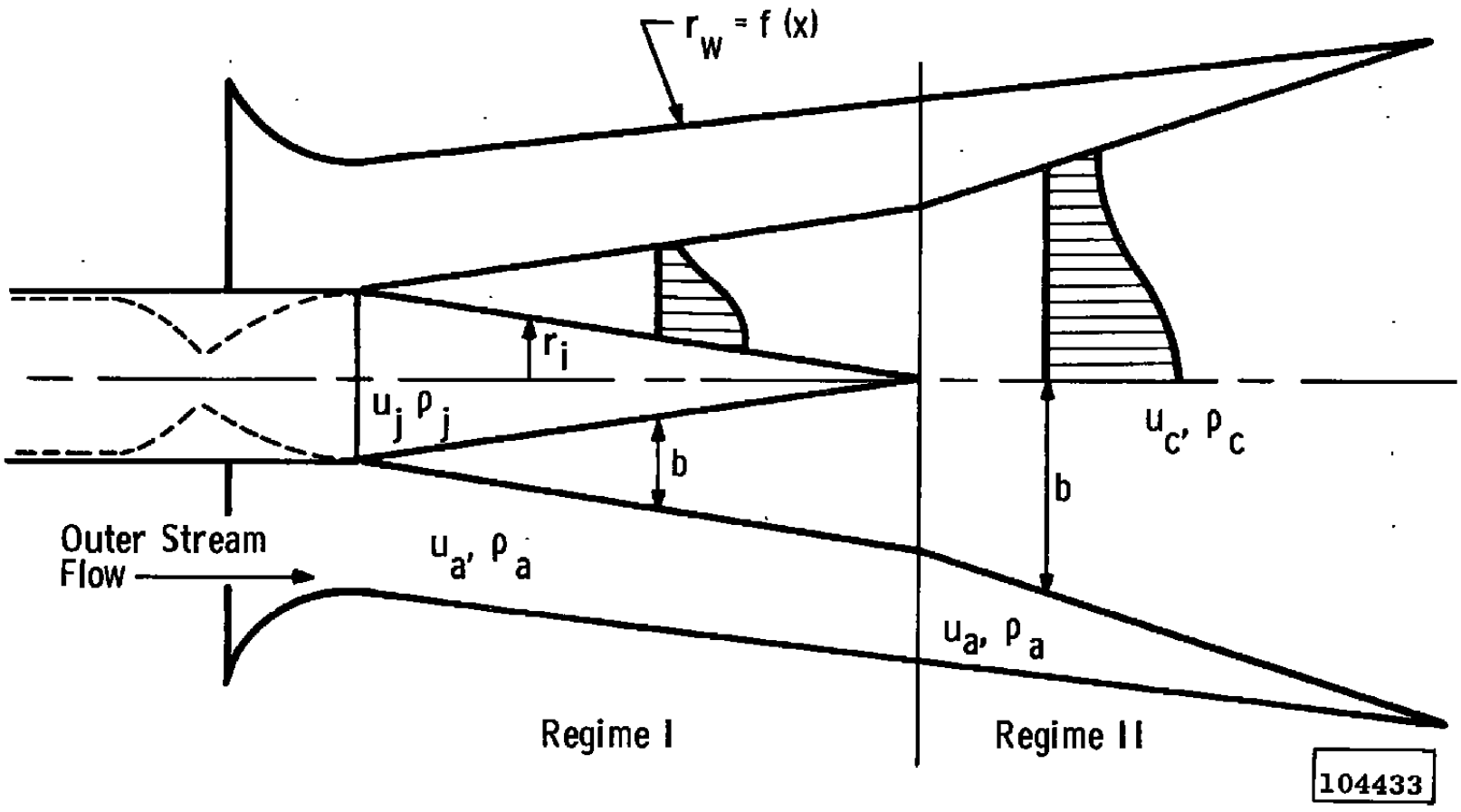

Fig. 3 Flow Model for First and Second Regimes

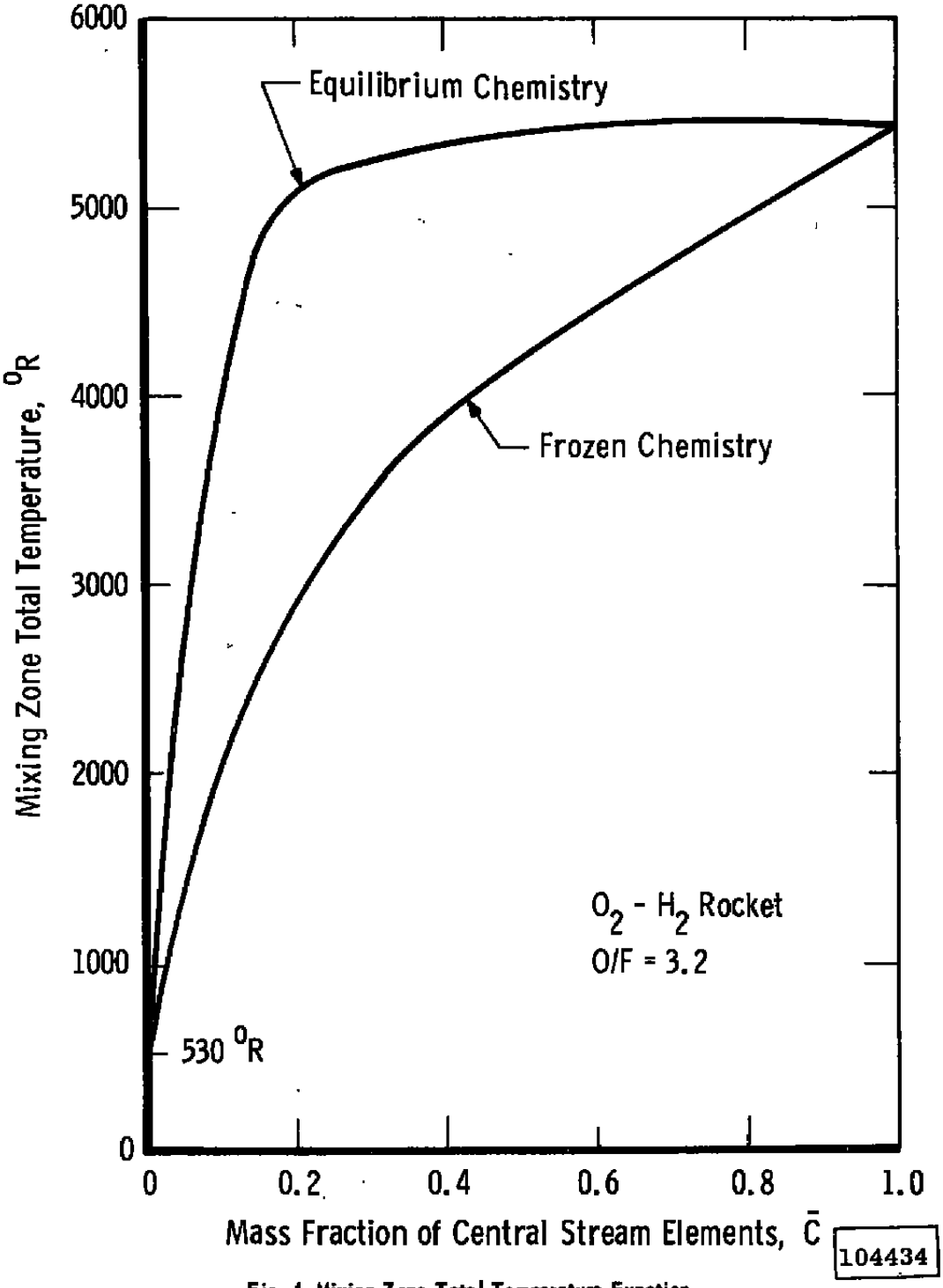

Fig. 4 Mixing Zone Total Temperature Function

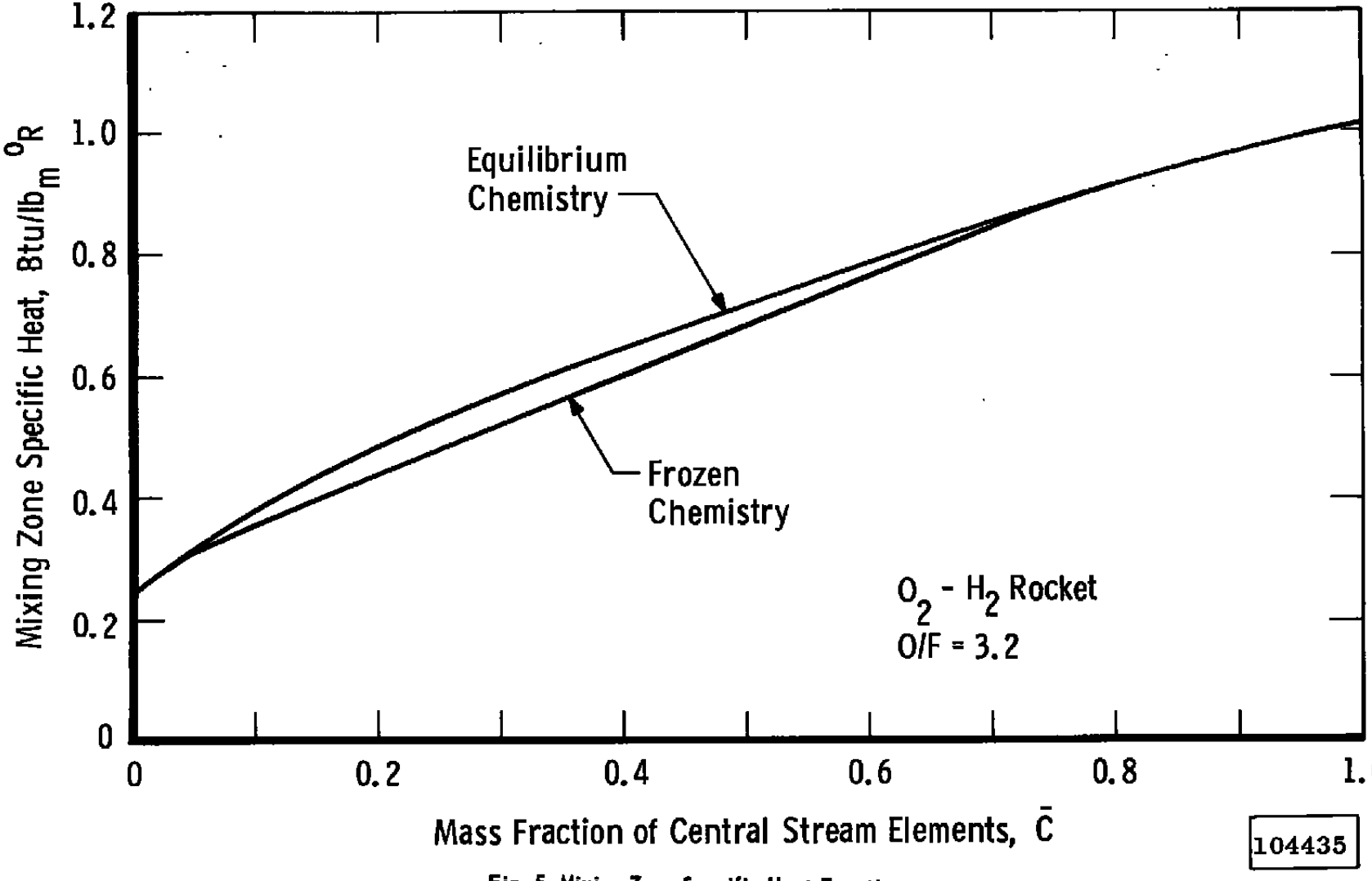

Fig. 5 Mixing Zone Specific Heat Function

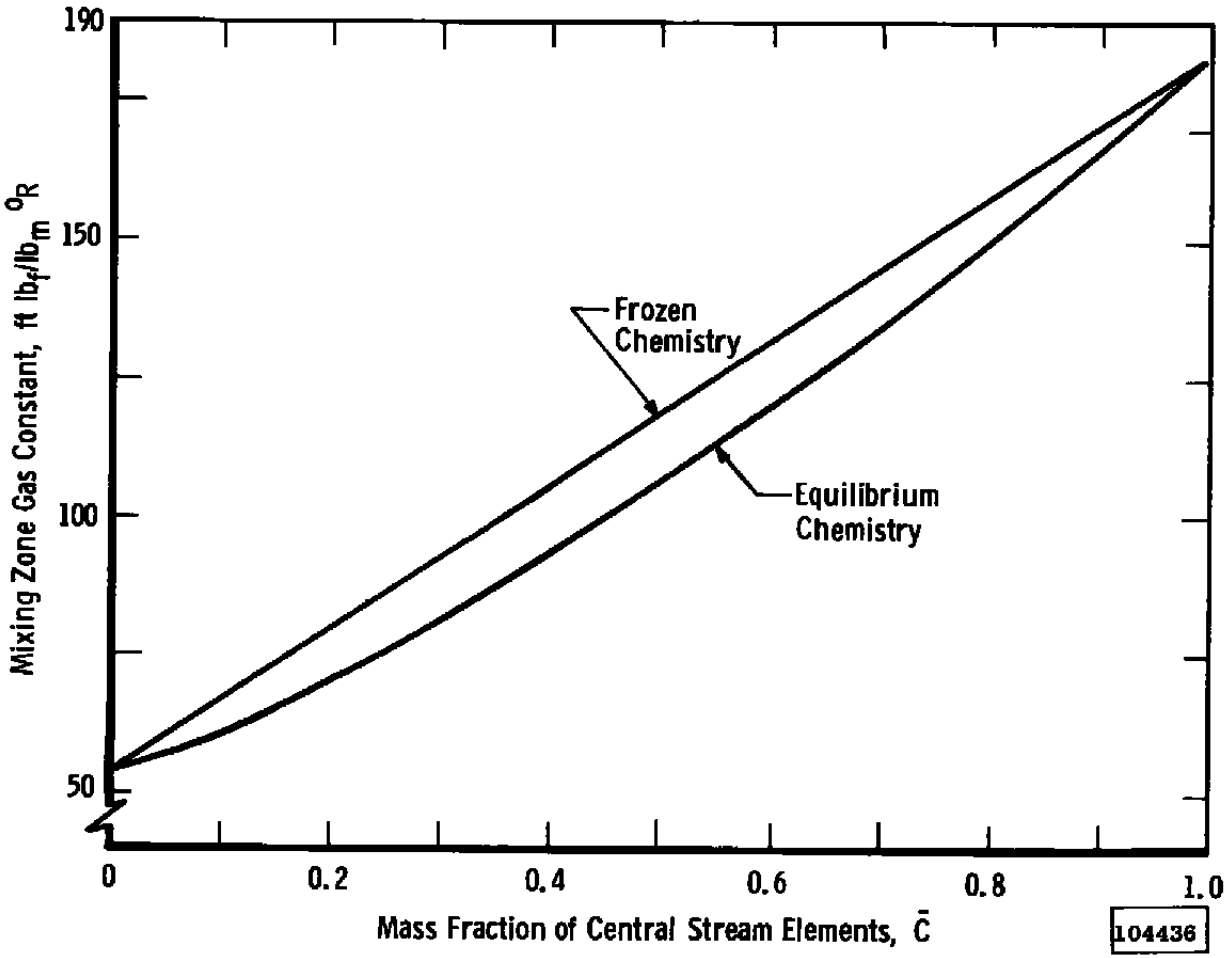

Fig. 6 Mixing Zone Gas Constant Function

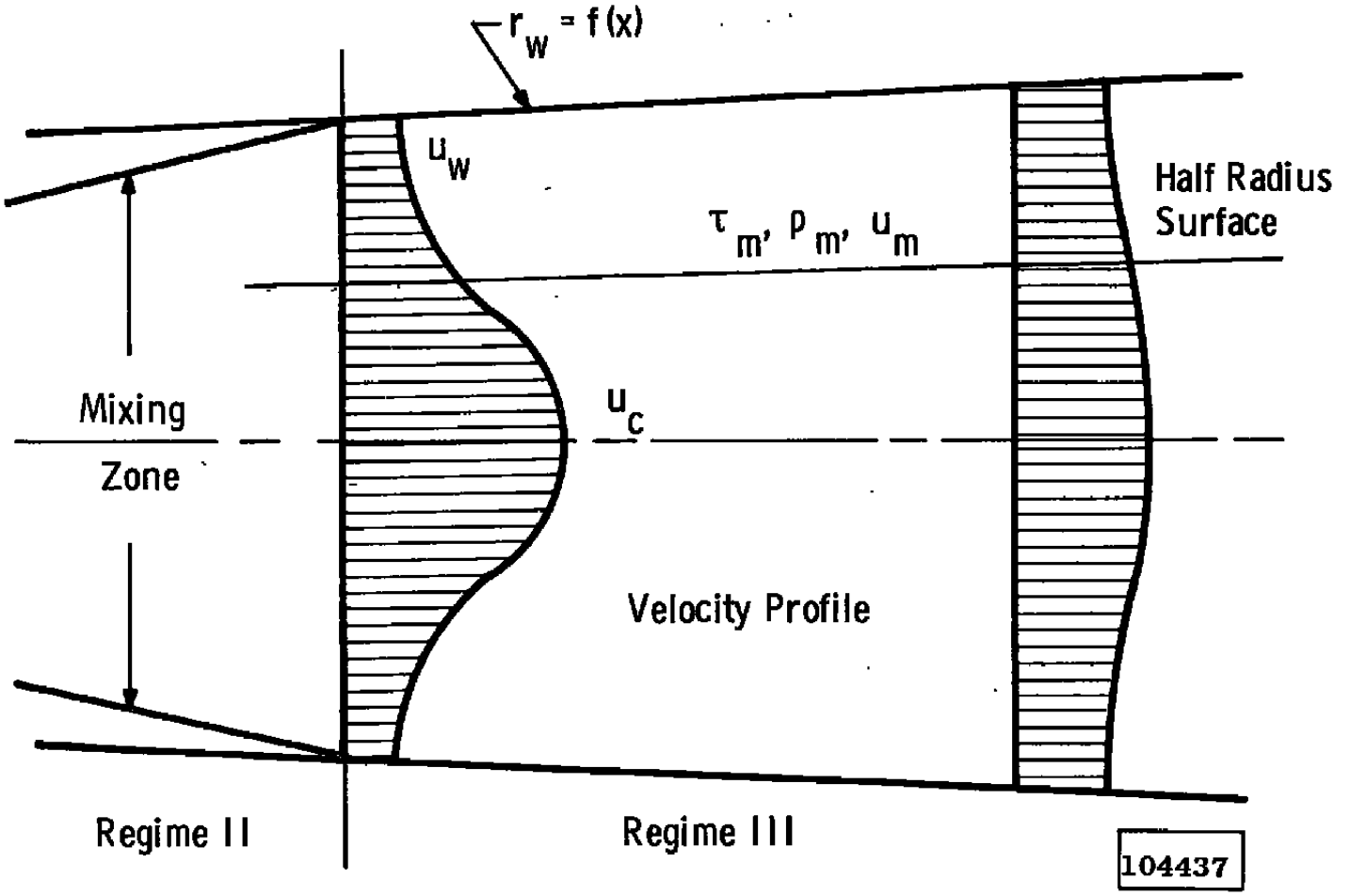

Fig. 7 Flow Model for Third Regime

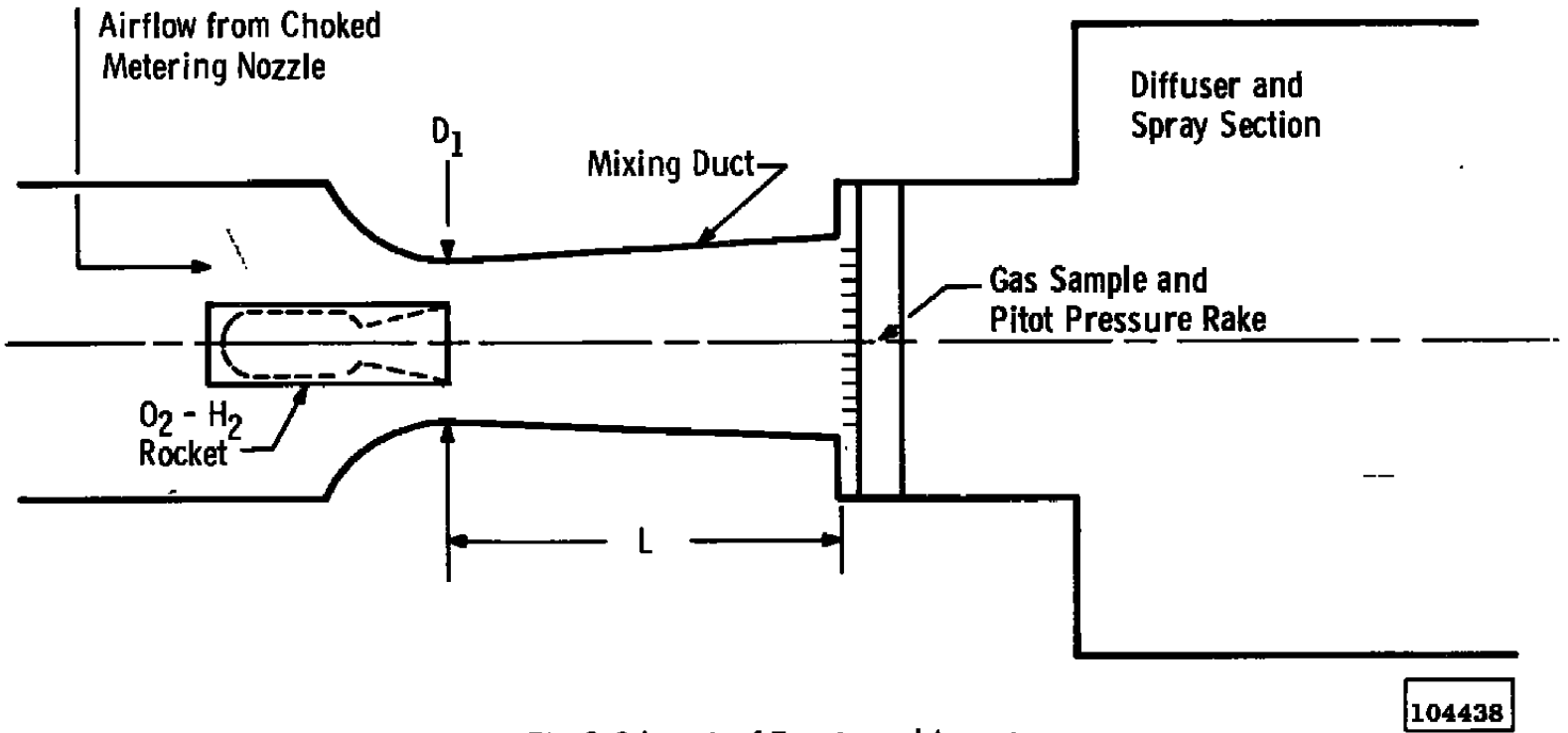

Fig. 8 Schematic of Experimental Apparatus

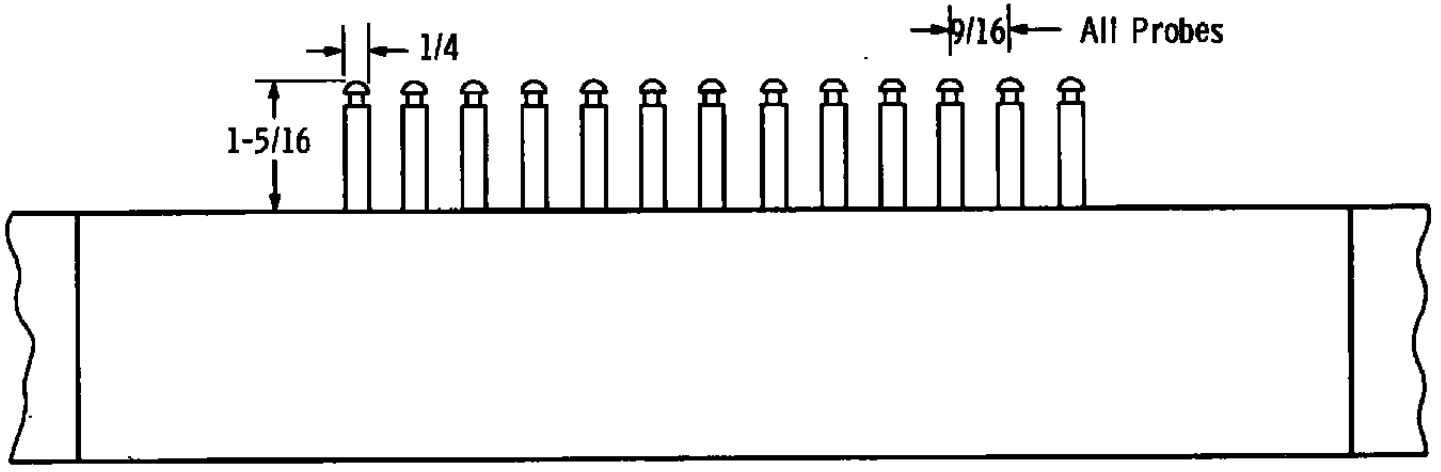

a. Rake Geometry

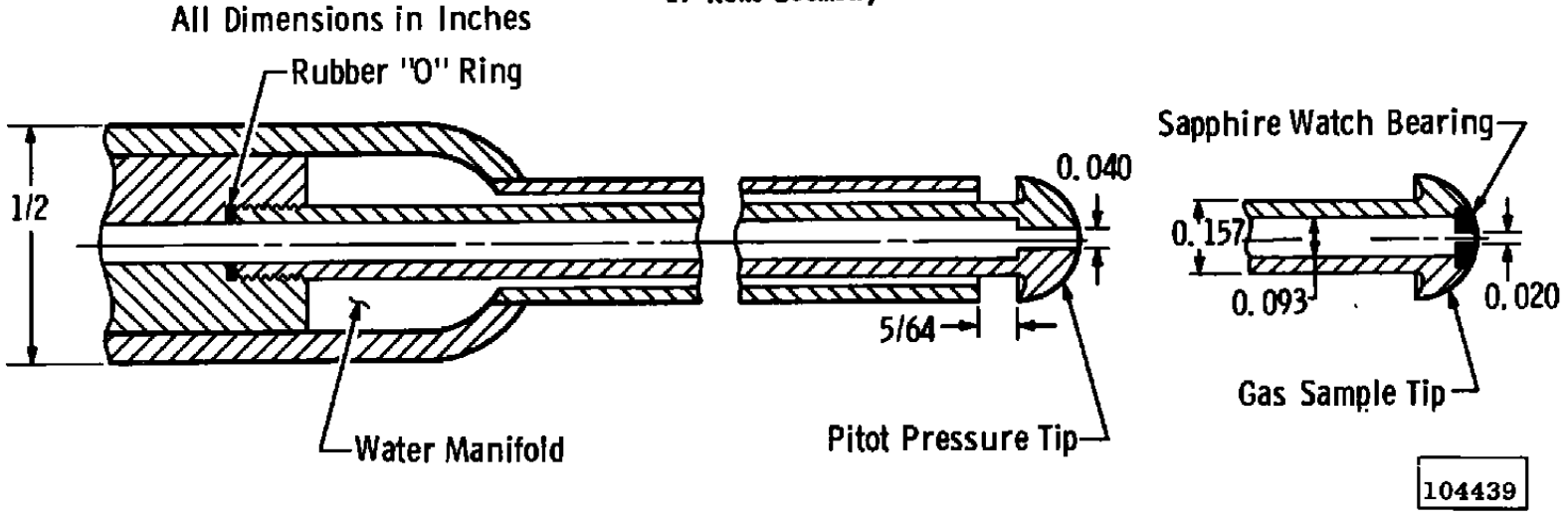

b. Probe Tip Details

Fig. 9 Survey Rake

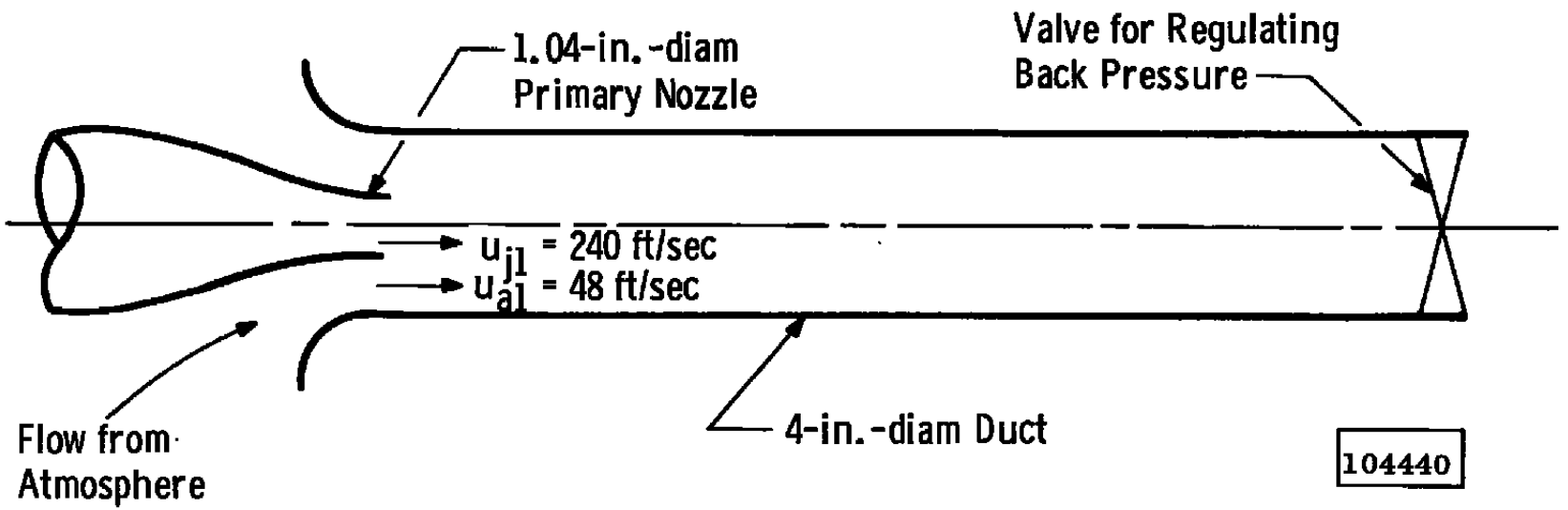

Fig. 10 Apparatus for Incompressible Experiments

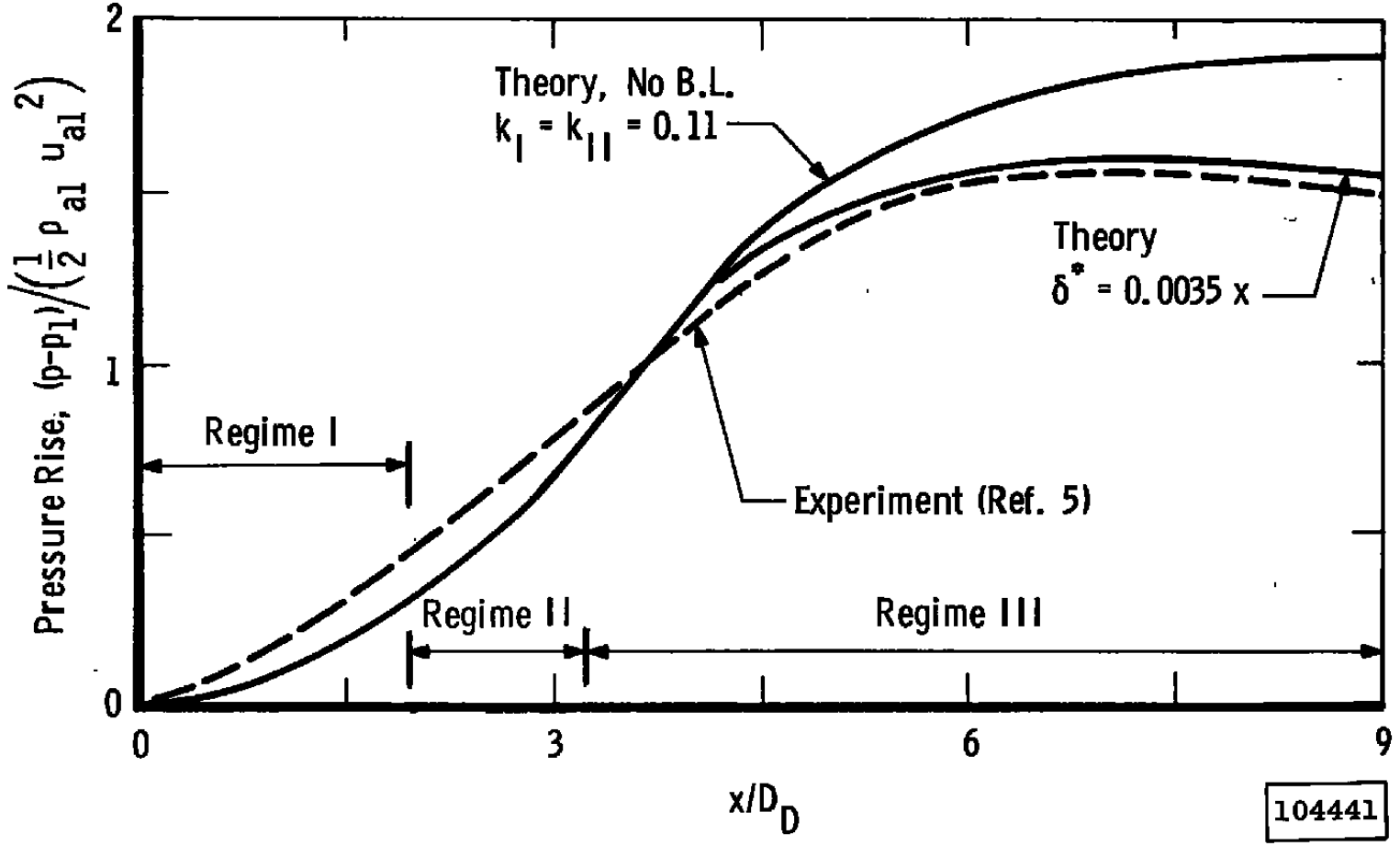

Fig. 11 Duct Pressure Distribution for Incompressible Mixing

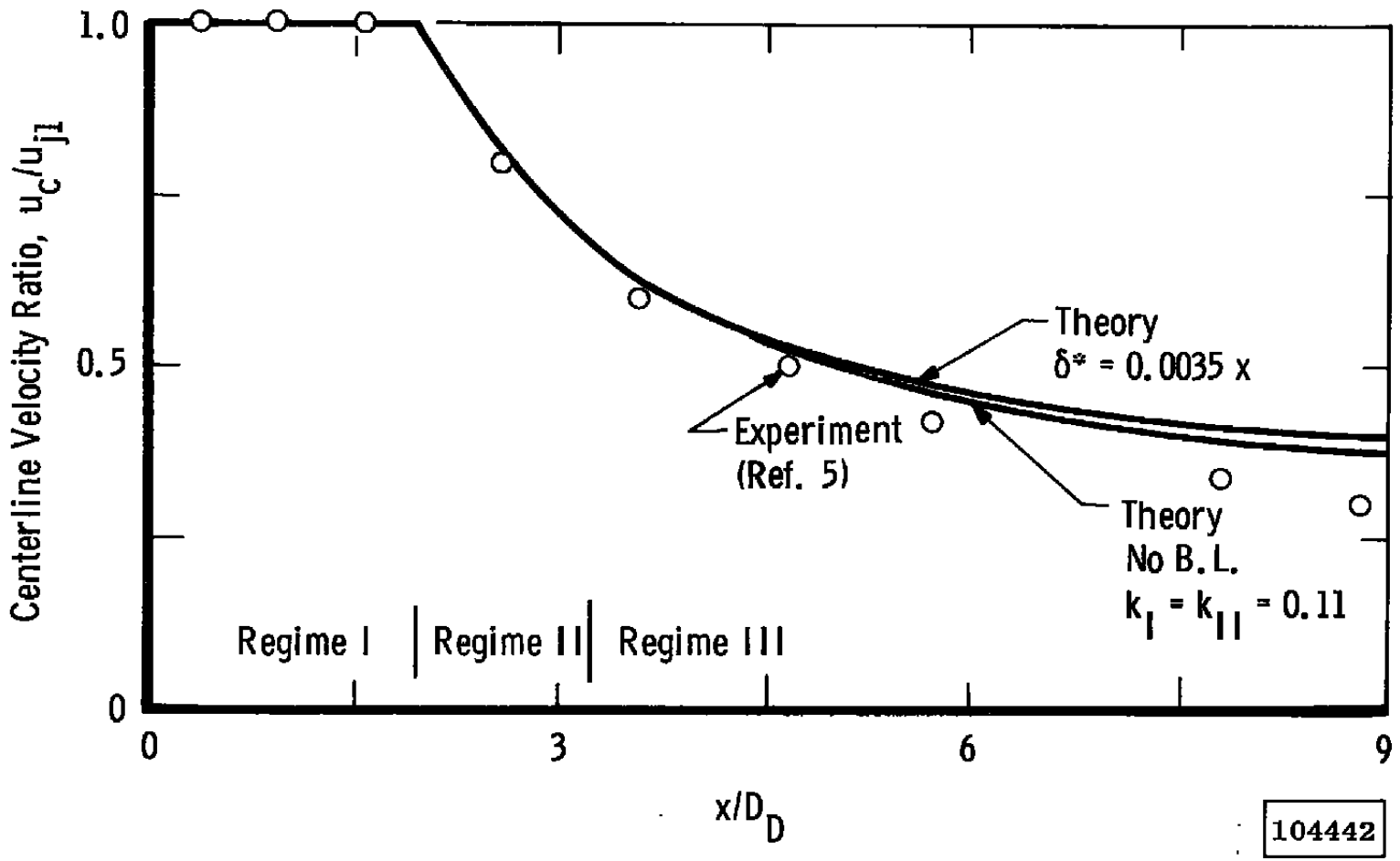

Fig. 12 Centerline Velocity for Incompressible Mixing

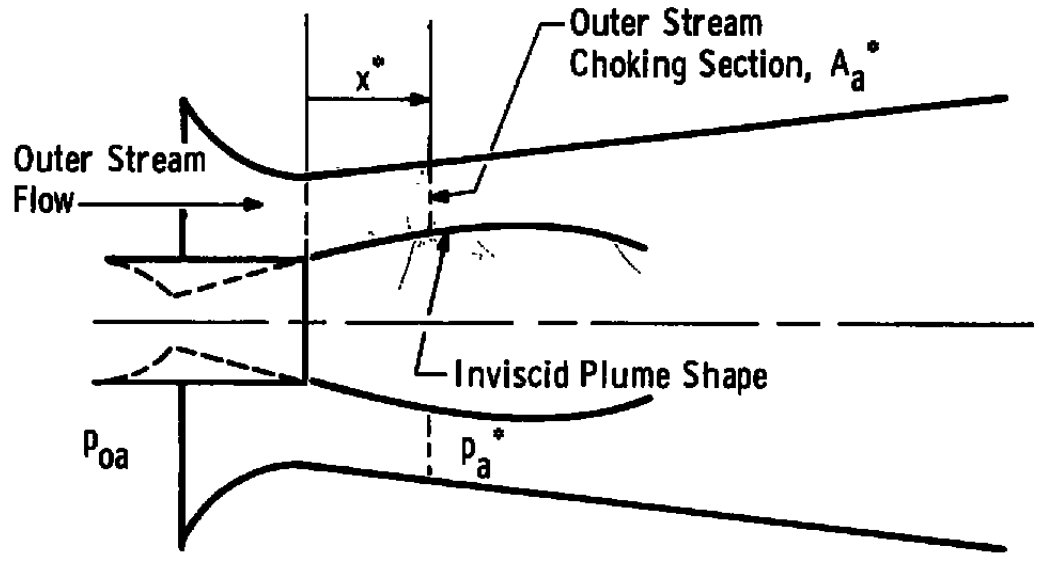

a. Schematic of Initial Rocket Pluming Effect

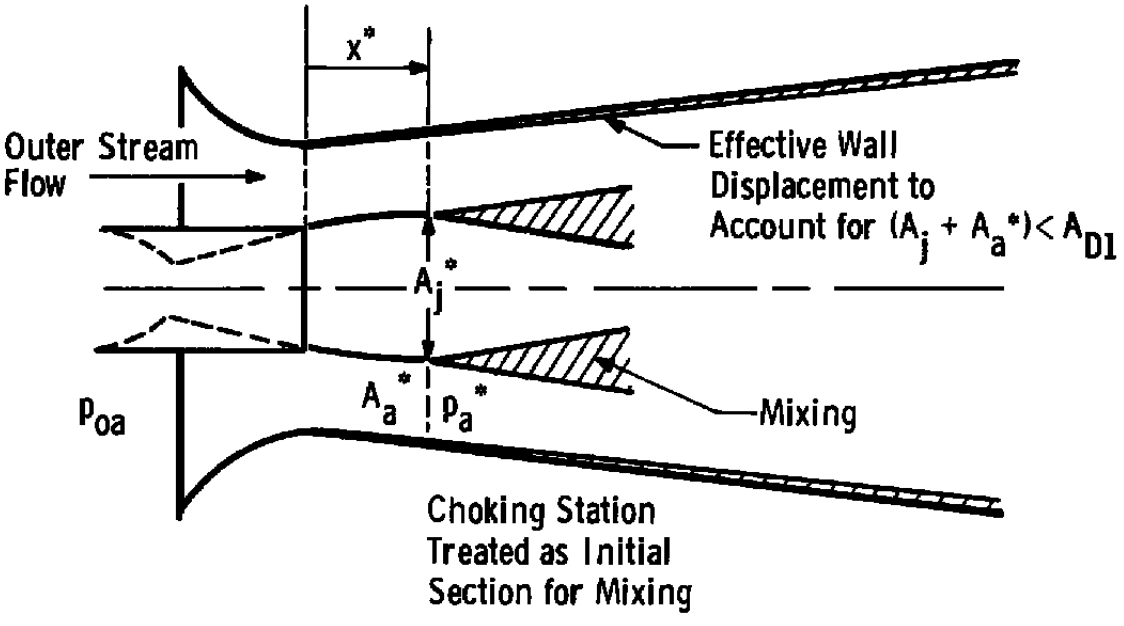

b. Approximate Treatment of Rocket Pluming

104443

Fig. 13 Initial Pluming of Rocket Jet

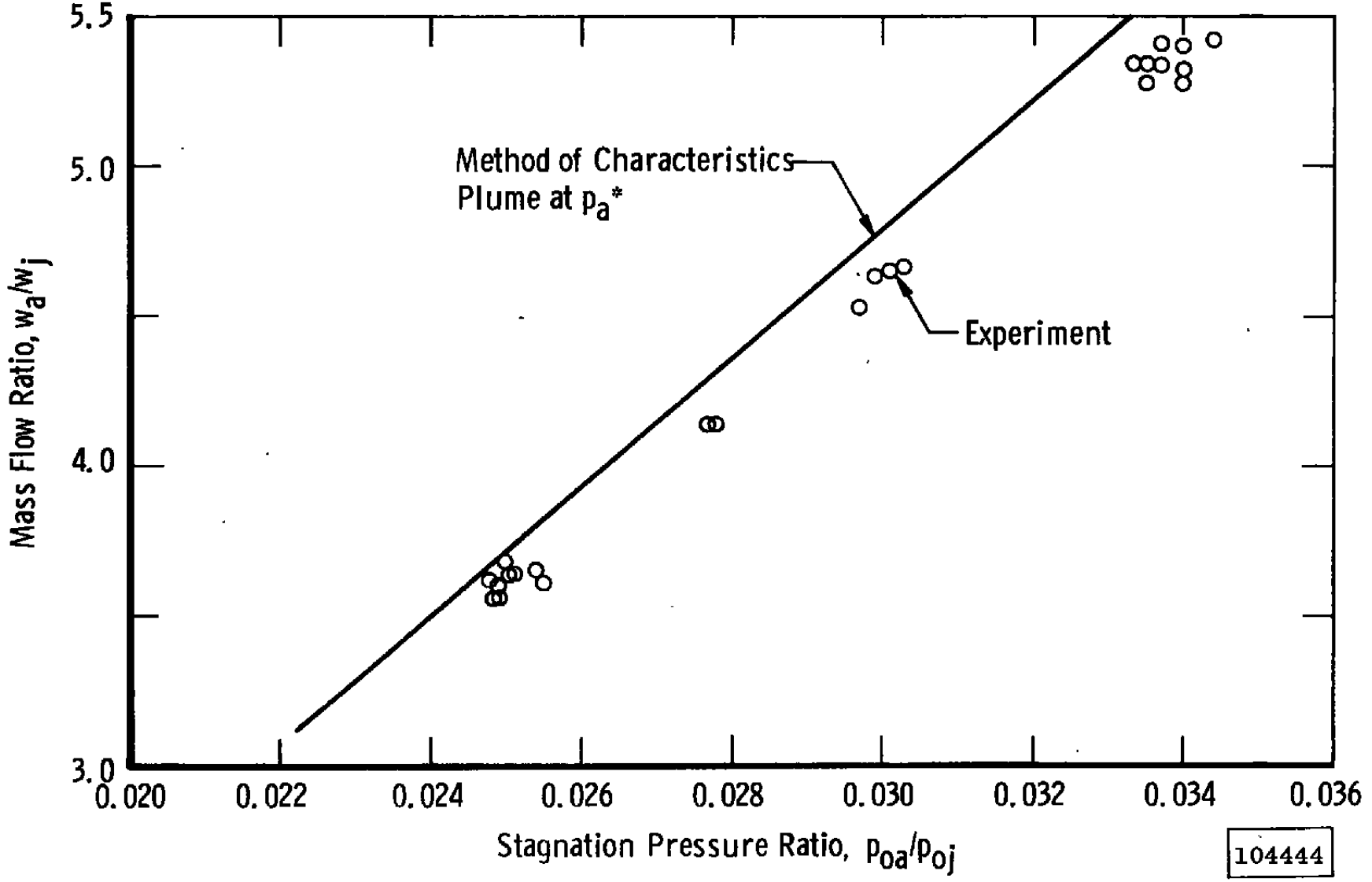

Fig. 14 Mass Flow Ratio (O_2-H_2 Rocket)

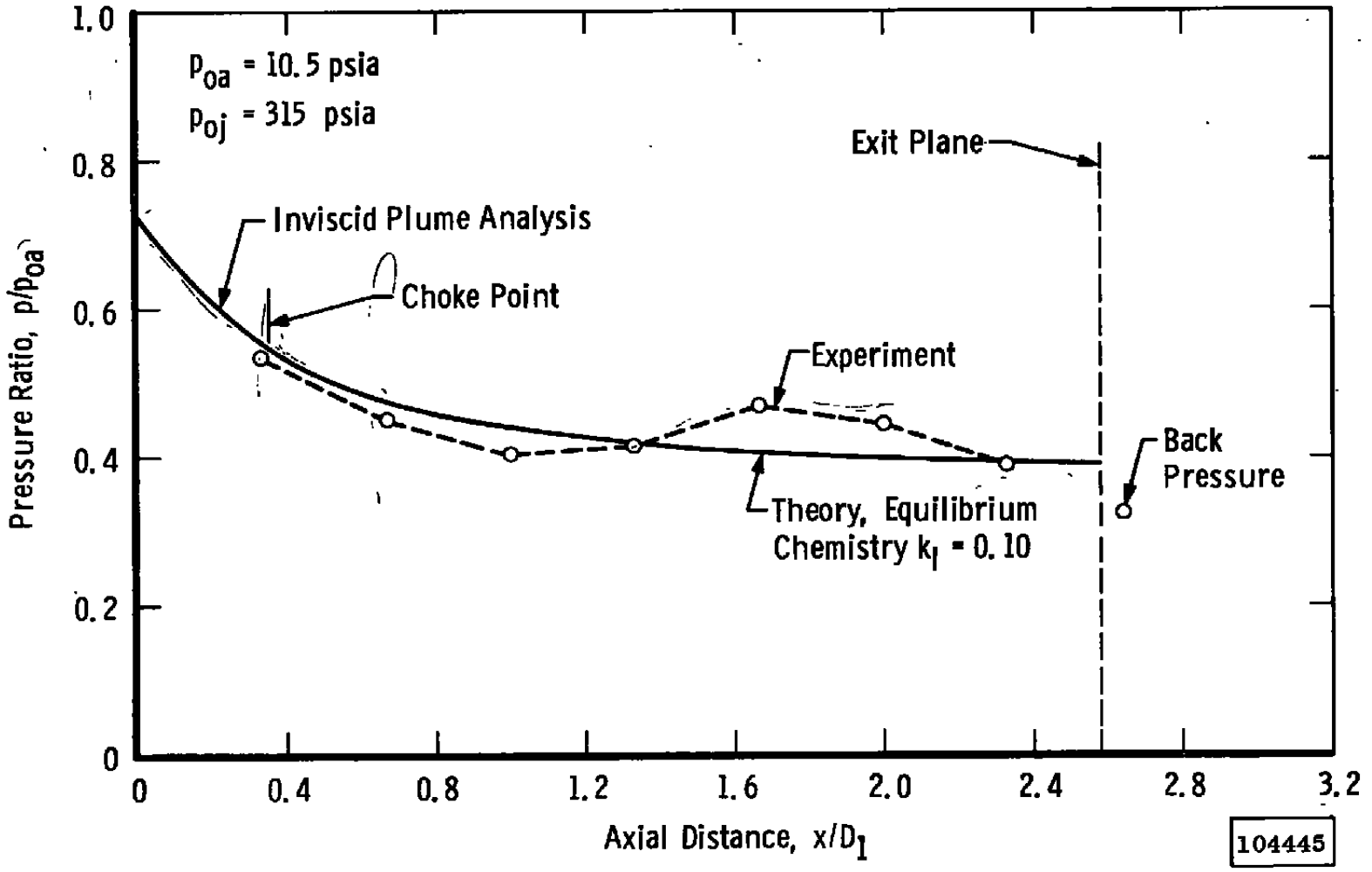

a. w_a/w_j = 5.3

Fig. 15 Duct Wall Pressure Distribution (O_2-H_2 Rocket)

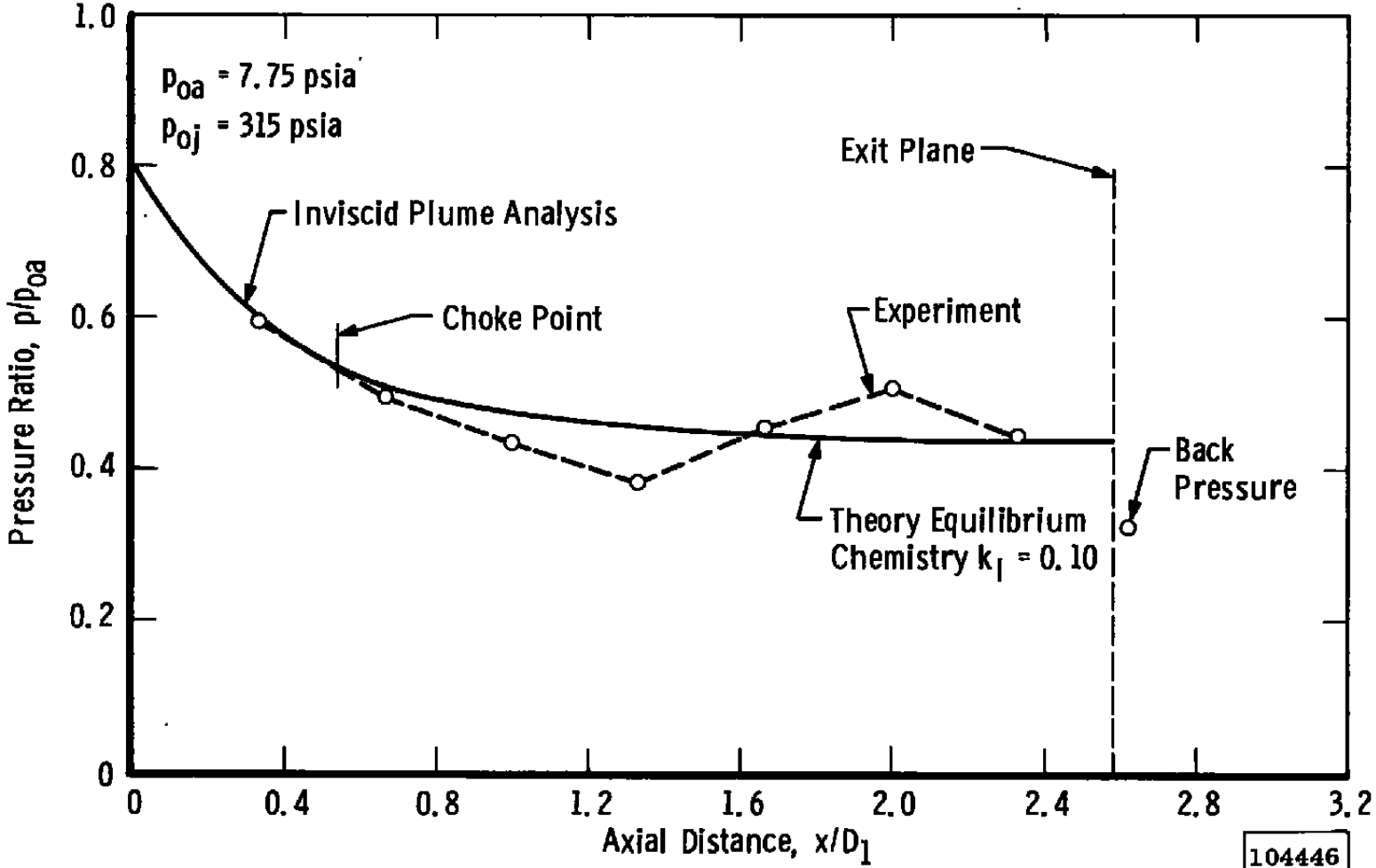

b. w_a/w_j = 3.6

Fig. 15 Concluded

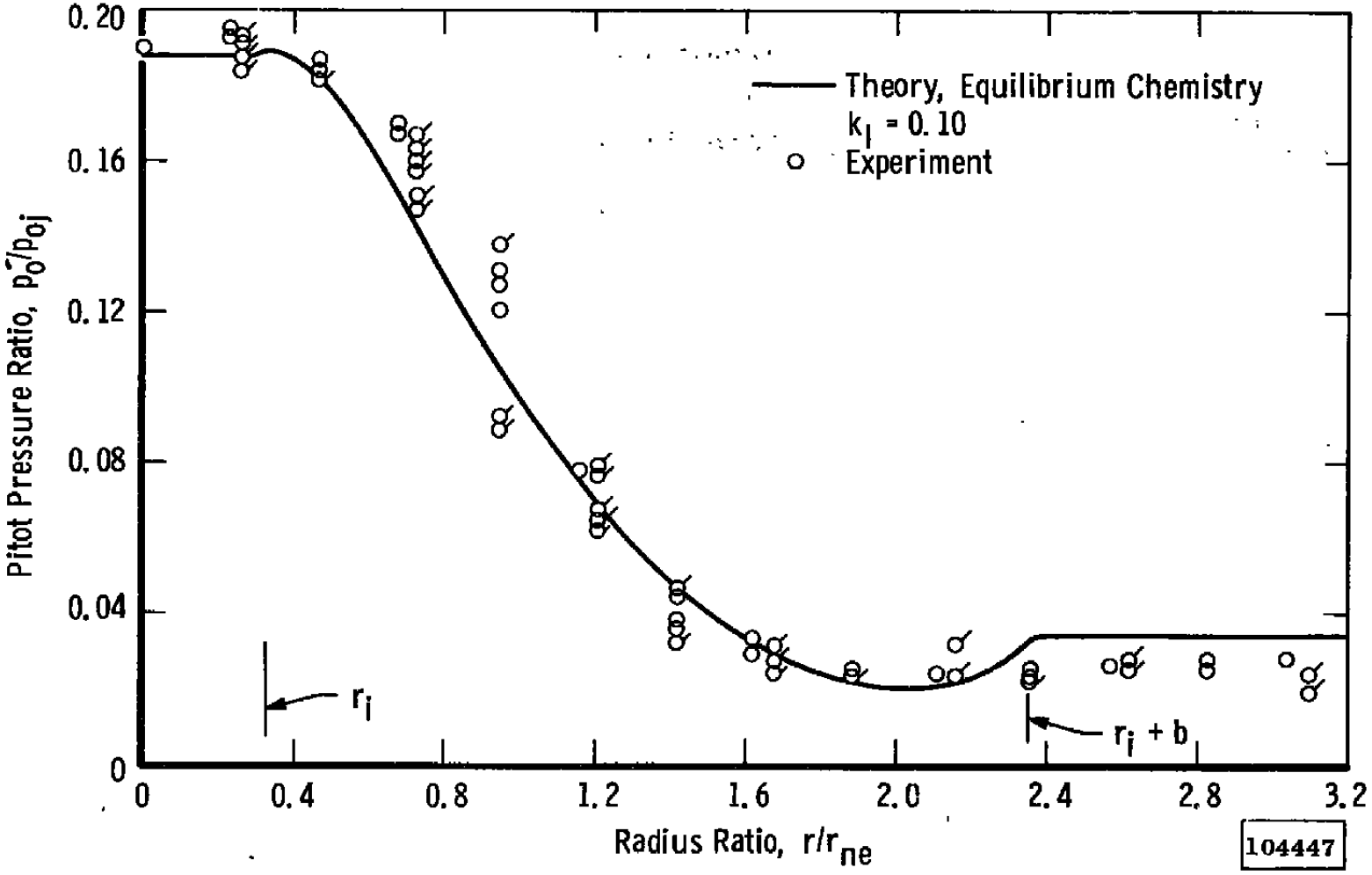

a. w_a/w_l = 5.3

Fig. 16 Radial Pitot Pressure Distribution at Duct Exit (O_2-H_2 Rocket)

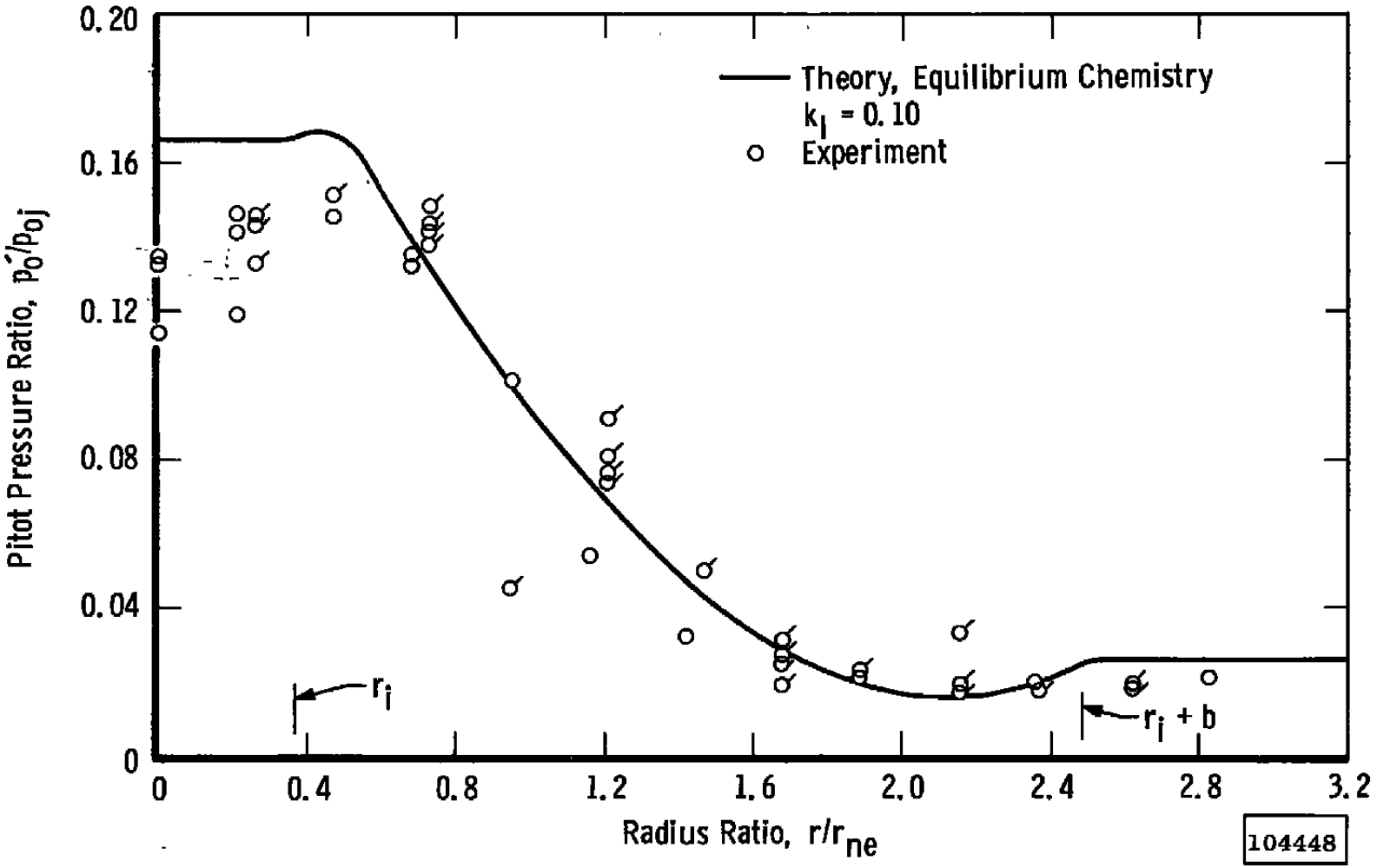

b. w_a/w_j = 3.6

Fig. 16 Concluded

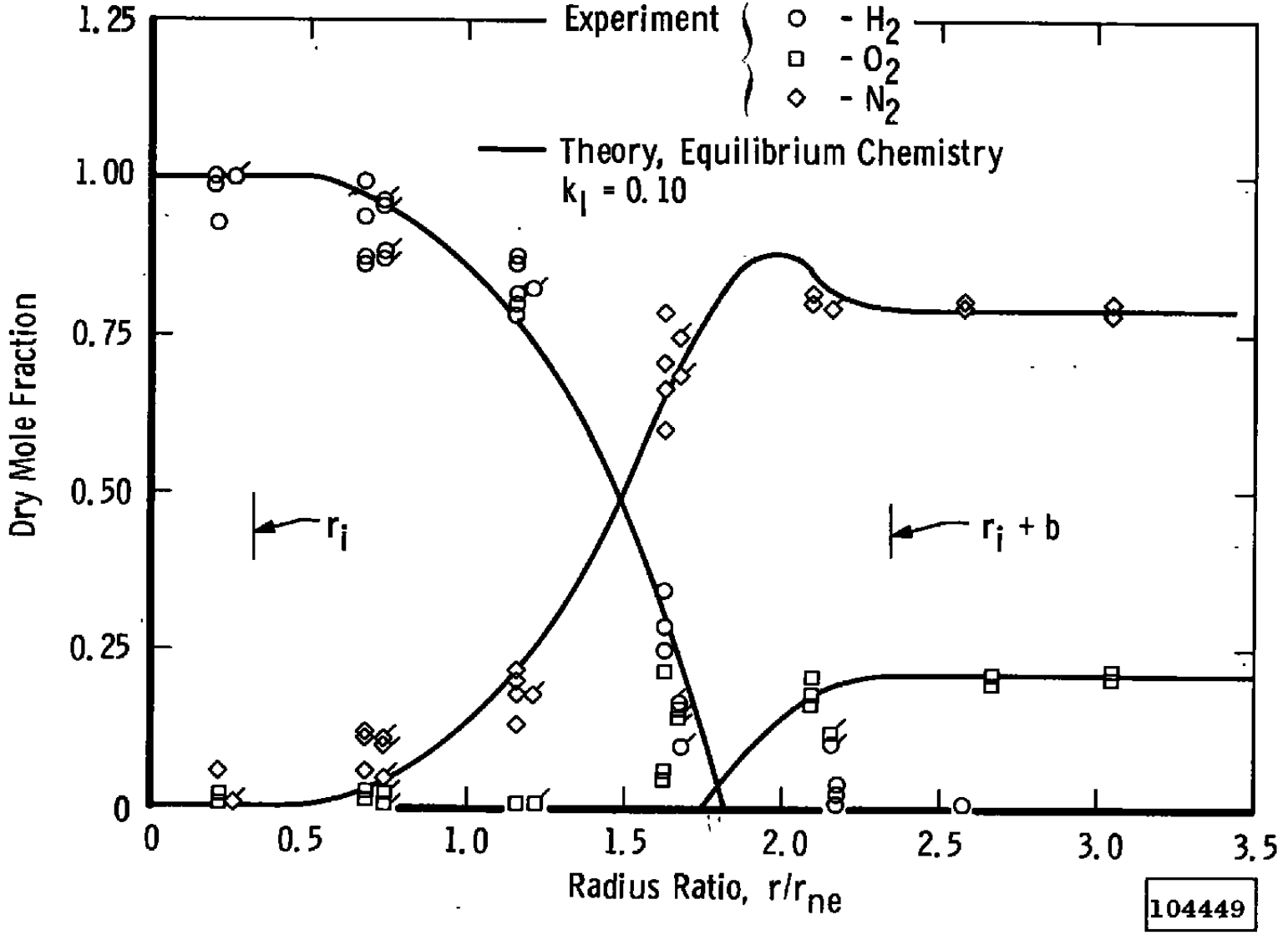

a. w_a/w_j = 5.3

Fig. 17 Radial Composition Distribution at Duct Exit (O_2-H_2 Rocket)

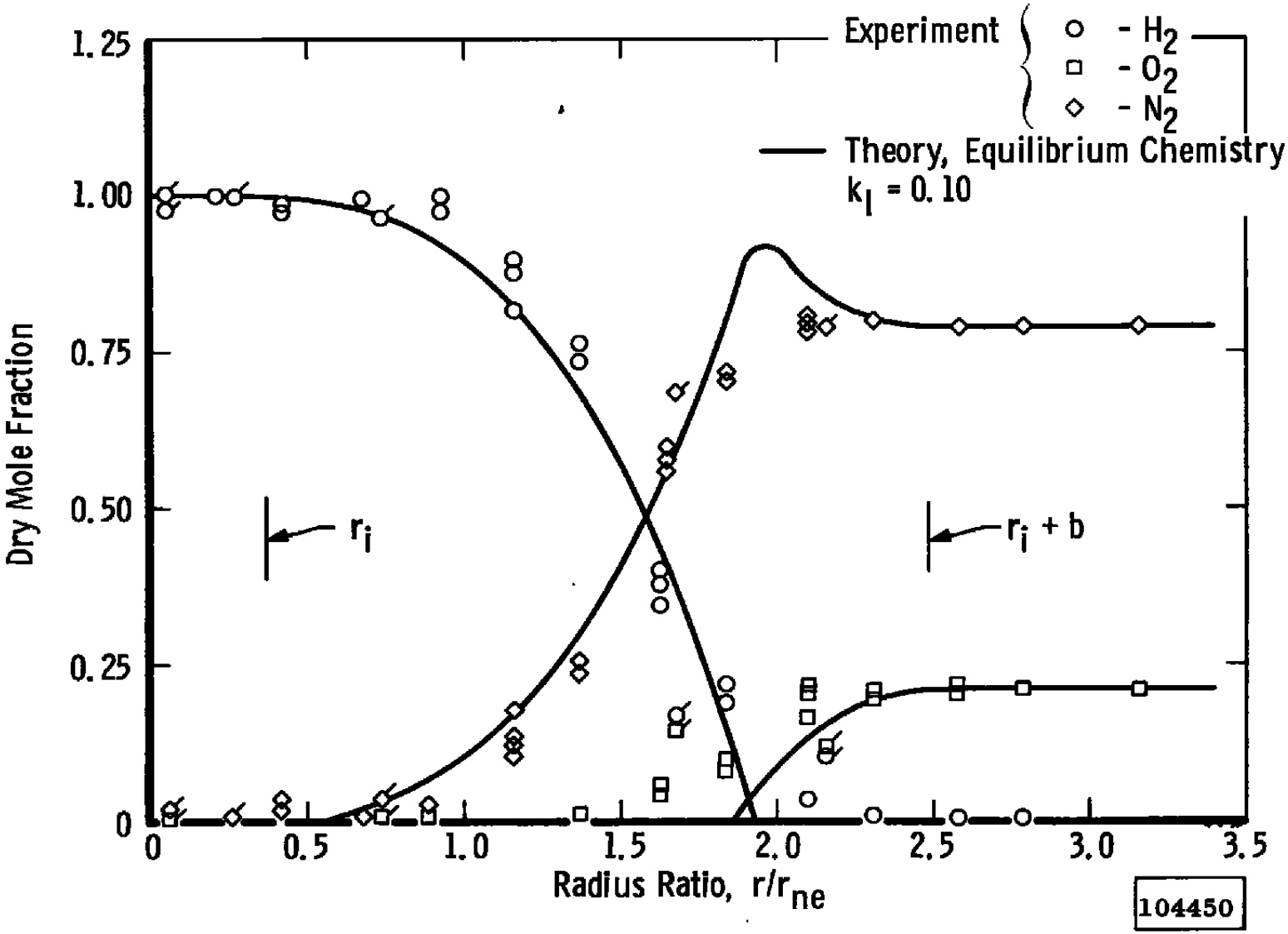

b. w_o/w_l = 3.6

Fig. 17 Concluded

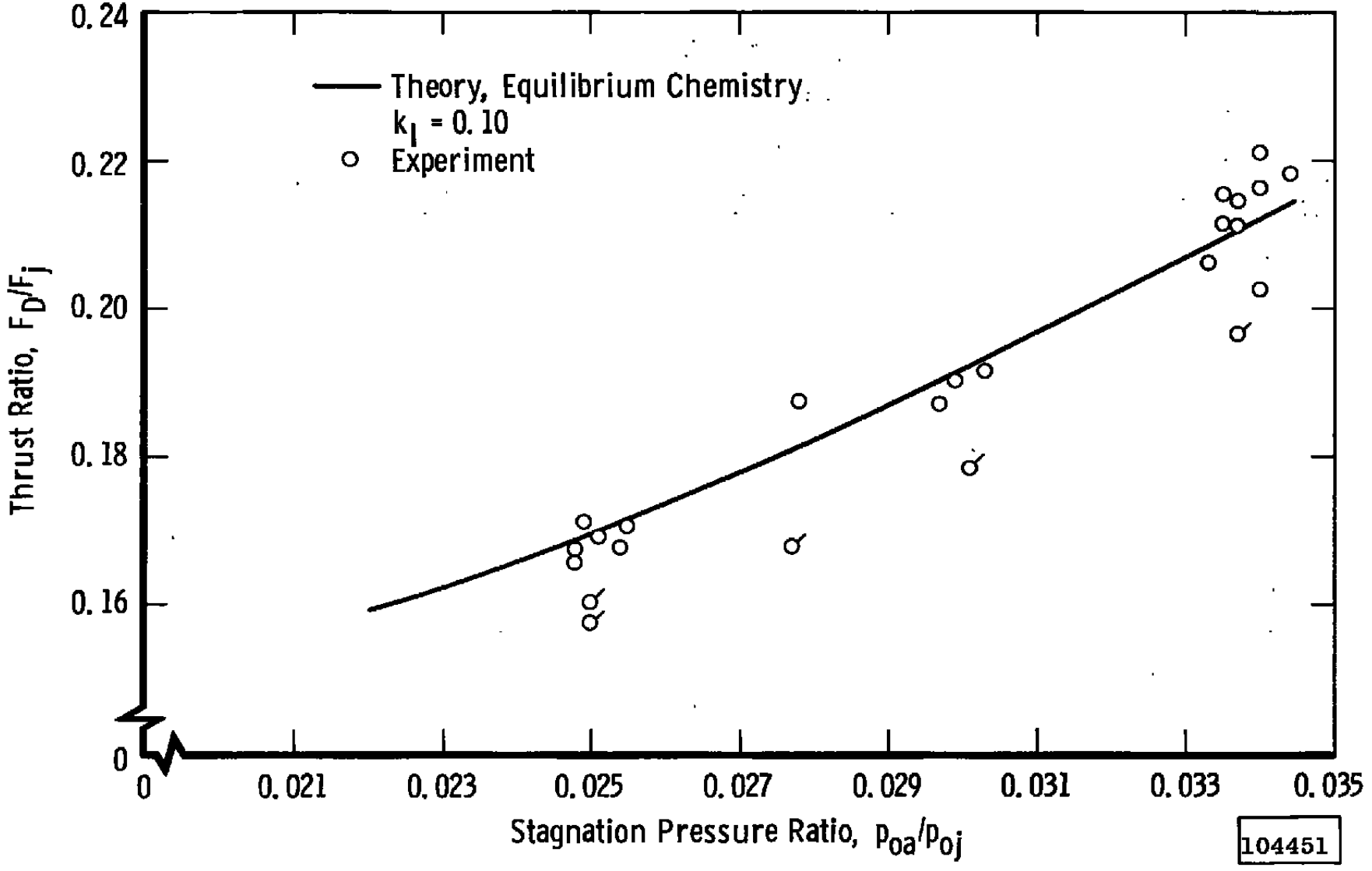

Fig. 18 Mixing Duct Thrust (O_2-H_2 Rocket)

TABLE I
EXPERIMENTAL PARAMETERS FOR MIXING AND BURNING APPARATUS

Nominal Rocket Parameters	
Oxidizer	Gaseous Oxygen
Fuel	Gaseous Hydrogen
Chamber Pressure (p_{oj})	315 psia
Calculated Vacuum Thrust (F_j)	391 lb_f
Characteristic Velocity (c^*)	8200 ft/sec
Mixture Ratio, by mass (O/F)	3.16 (±3 percent)
Total Propellant Mass Flow (w_j)	0.97 lb_m/sec
Throat Diameter	1.00 in.
Nozzle Exit Radius (r_{NE})	1.19 in.
Nozzle Configuration	15-deg; half-angle, conical
Mixing Duct	
Inlet Diameter (D_i)	6 in.
Length (L)	15.5 in.
Divergence half-angle	3 deg
Nominal Air Temperature (T_{oa})	530°R

UNCLASSIFIED

Security Classification

DOCUMENT CONTROL DATA - R&D

(Security classification of title, body of abstract and indexing annotation must be entered when the overall report is classified)

1 ORIGINATING ACTIVITY *(Corporate author)*
Arnold Engineering Development Center
ARO, Inc., Operating Contractor
Arnold Air Force Station, Tennessee

2a REPORT SECURITY CLASSIFICATION
UNCLASSIFIED

2b GROUP
N/A

3 REPORT TITLE
MIXING AND BURNING OF BOUNDED COAXIAL STREAMS

4 DESCRIPTIVE NOTES *(Type of report and inclusive dates)*
N/A

5 AUTHOR(S) *(Last name, first name, initial)*
Peters, C. E., Peters, T., and Billings, R. B., ARO, Inc.

6. REPORT DATE	7a. TOTAL NO. OF PAGES	7b. NO OF REFS
MARCH 1965	51	13

8a. CONTRACT OR GRANT NO.	9a. ORIGINATOR'S REPORT NUMBER(S)
AF 40(600)-1000 b. PROJECT NO. 6950 c. Program Element 62405184 d. Task 695002	AEDC-TR-65-4
	9b. OTHER REPORT NO(S) *(Any other numbers that may be assigned this report)* N/A

10. AVAILABILITY/LIMITATION NOTICES
Qualified requesters may obtain copies of this report from DDC.

11. SUPPLEMENTARY NOTES	12. SPONSORING MILITARY ACTIVITY
N/A	Arnold Engineering Development Center, Air Force Systems Command, Arnold Air Force Station, Tennessee

13 ABSTRACT

An experimental and theoretical investigation of bounded turbulent mixing with chemical reactions is described. Configurations which are applicable to the air-augmented rocket are considered. Experimental results are presented for a mixing apparatus in which a fuel-rich O_2-H_2 rocket stream was mixed with a secondary airstream inside a conical duct. An integral mixing theory is described, in which conservation equations are satisfied across the duct. The inviscid portions of the duct flow are considered one-dimensional, and the mixing zone profiles are assumed to exhibit shape similarity. The theory is extended to include the downstream regime where the mixing region extends across the entire duct. Correlations of the theory with incompressible and reactive compressible mixing experiments indicate that the theory provides a satisfactory overall representation of the bounded mixing process.

DD FORM 1 JAN 64 1473

UNCLASSIFIED

Security Classification

14 KEY WORDS	LINK A		LINK B		LINK C	
	ROLE	WT	ROLE	WT	ROLE	WT
jet mixing						
bounded mixing						
chemical reactions						
turbulence						
coaxial streams						
air-augmented rockets						

INSTRUCTIONS

1. ORIGINATING ACTIVITY: Enter the name and address of the contractor, subcontractor, grantee, Department of Defense activity or other organization *(corporate author)* issuing the report.

2a. REPORT SECURITY CLASSIFICATION: Enter the overall security classification of the report. Indicate whether "Restricted Data" is included. Marking is to be in accordance with appropriate security regulations.

2b. GROUP: Automatic downgrading is specified in DoD Directive 5200.10 and Armed Forces Industrial Manual. Enter the group number. Also, when applicable, show that optional markings have been used for Group 3 and Group 4 as authorized.

3. REPORT TITLE: Enter the complete report title in all capital letters. Titles in all cases should be unclassified. If a meaningful title cannot be selected without classification, show title classification in all capitals in parenthesis immediately following the title.

4. DESCRIPTIVE NOTES: If appropriate, enter the type of report, e.g., interim, progress, summary, annual, or final. Give the inclusive dates when a specific reporting period is covered.

5. AUTHOR(S): Enter the name(s) of author(s) as shown on or in the report. Enter last name, first name, middle initial. If military, show rank and branch of service. The name of the principal author is an absolute minimum requirement.

6. REPORT DATE: Enter the date of the report as day, month, year, or month, year. If more than one date appears on the report, use date of publication.

7a. TOTAL NUMBER OF PAGES: The total page count should follow normal pagination procedures, i.e., enter the number of pages containing information.

7b. NUMBER OF REFERENCES: Enter the total number of references cited in the report.

8a. CONTRACT OR GRANT NUMBER: If appropriate, enter the applicable number of the contract or grant under which the report was written.

8b, 8c, & 8d. PROJECT NUMBER: Enter the appropriate military department identification, such as project number, subproject number, system numbers, task number, etc.

9a. ORIGINATOR'S REPORT NUMBER(S): Enter the official report number by which the document will be identified and controlled by the originating activity. This number must be unique to this report.

9b. OTHER REPORT NUMBER(S): If the report has been assigned any other report numbers *(either by the originator or by the sponsor)*, also enter this number(s).

10. AVAILABILITY/LIMITATION NOTICES: Enter any limitations on further dissemination of the report, other than those imposed by security classification, using standard statements such as:

(1) "Qualified requesters may obtain copies of this report from DDC."

(2) "Foreign announcement and dissemination of this report by DDC is not authorized."

(3) "U. S. Government agencies may obtain copies of this report directly from DDC. Other qualified DDC users shall request through

_____."

(4) "U. S. military agencies may obtain copies of this report directly from DDC. Other qualified users shall request through

_____."

(5) "All distribution of this report is controlled. Qualified DDC users shall request through

_____."

If the report has been furnished to the Office of Technical Services, Department of Commerce, for sale to the public, indicate this fact and enter the price, if known.

11. SUPPLEMENTARY NOTES: Use for additional explanatory notes.

12. SPONSORING MILITARY ACTIVITY: Enter the name of the departmental project office or laboratory sponsoring *(paying for)* the research and development. Include address.

13. ABSTRACT: Enter an abstract giving a brief and factual summary of the document indicative of the report, even though it may also appear elsewhere in the body of the technical report. If additional space is required, a continuation sheet shall be attached.

It is highly desirable that the abstract of classified reports be unclassified. Each paragraph of the abstract shall end with an indication of the military security classification of the information in the paragraph, represented as *(TS)*, *(S)*, *(C)*, or *(U)*.

There is no limitation on the length of the abstract. However, the suggested length is from 150 to 225 words.

14. KEY WORDS: Key words are technically meaningful terms or short phrases that characterize a report and may be used as index entries for cataloging the report. Key words must be selected so that no security classification is required. Identifiers, such as equipment model designation, trade name, military project code name, geographic location, may be used as key words but will be followed by an indication of technical context. The assignment of links, rules, and weights is optional.